Chapter 5

EVOLUTIONARY MORPHOLOGY

The subject of biological diversity [SEE SECTION 8.1] is often conveyed with the question: Why are there so many kinds of organisms? We may just as well turn this question around, however, and ask why there are so *few* kinds. In discussing the nature of populations and species in Chapter 3, we saw that form is not randomly or uniformly distributed, but rather that organisms form more or less discrete units. Form is also nonrandomly distributed at higher taxonomic levels. The species that have lived on the earth represent a very small subset of all imaginable forms. In other words, most forms that are conceivable have not in fact evolved. By contrast, some aspects of form have evolved numerous times convergently [SEE SECTION 4.2]. Given that life has been evolving on earth for well over three billion years, why is the spectrum of biologic form so limited?

Broadly speaking, **evolutionary morphology** is concerned with understanding the diversity and the nonrandomness of form. This is obviously an enormous subject. We will emphasize two main aspects of this area of research: **functional morphology,** which interprets the function of organisms in relation to their form, and **theoretical morphology,** which compares the spectrum of conceivable forms to those that have actually evolved.

5.1 ADAPTATION AND OTHER UNDERLYING ASSUMPTIONS

We usually start with the working assumption that the distribution of form can largely be explained by **adaptation.** The distinction can be made between adaptation as a state (the fit between an organism's form and physiology and its environment and way of life) and adaptation as a process (the evolutionary mechanisms and pathways that produce adaptive traits in a lineage). This distinction is most relevant when there have been evolutionary shifts in function. Natural selection may have produced a structure to perform a particular function in a particular environment, and the structure may have been subsequently co-opted and modified, over evolutionary time, to suit a new functional need.

A persuasive example of such a functional shift is found in the wings of insects. Insect wings must exceed a critical size to generate flight. Because it is practically impossible that fully developed wings were produced by genetic mutation in a single step, the earliest stages in the evolution of the wing must have been small organs that could not have been used for flight. In other words, it seems unlikely that the wing initially evolved by natural selection for the function of flight.

This does not mean that a small, winglike structure would have been useless, however. Functional modeling of the kind we discuss later in this chapter has shown that small, winglike appendages can be useful in regulating body temperature by absorbing solar radiation. In a series of experiments carried out by biologists J. Kingsolver and M. Koehl (1985), wings attached to model insects became more effective at thermoregulation as they were made larger, but only up to a certain size. Above that size, the wings began to generate appreciable lift and to confer other aerodynamic benefits to the models. This suggests that natural selection for the function of thermoregulation could have produced a wing sufficiently large that selection for the new function of flight could have taken over.

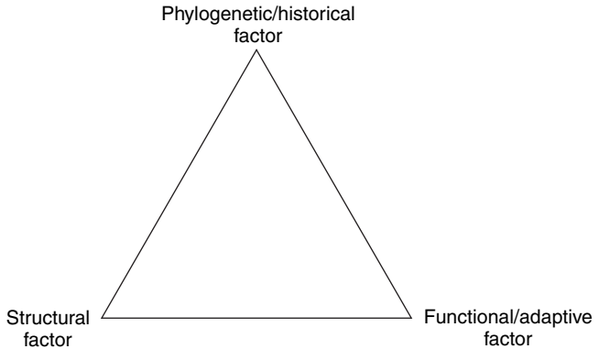

FIGURE 5.1 Schematic diagram depicting principal factors that contribute to biologic form, using the model of a ternary diagram familiar to geologists. Every form represents an interplay between immediate adaptation (functional factor), phylogenetic history, and constraints imposed by physical law and the properties of materials (structural factor). *(After Seilacher, 1970)*

In interpreting form, it is useful to consider a framework that distinguishes two major determinants of form in addition to adaptation (Figure 5.1). This framework, which has been developed extensively by the paleontologist Adolf Seilacher and his colleagues, is commonly referred to as **constructional morphology.** The **historical** or **phylogenetic factor** reflects those aspects of form that tend to be fixed within a biologic group because of their shared ancestry. For example, in interpreting the form of a specialized bivalve such as a scallop, we do not ask why it has two valves. This is a fundamental part of the bivalve body plan, one that did not vary in the history of the scallop lineage. Whether we interpret an aspect of form to reflect phylogenetic inheritance depends on the scale of analysis. In studying the *origin* of bivalve molluscs, we might well consider the adaptive value of having two valves; the **functional factor** might then be quite prominent.

The **structural factor** may be the least familiar, although it was discussed at great length by D'Arcy Thompson in his book *On Growth and Form* (1942) [SEE SECTION 2.3]. This factor pertains to consequences of physical law and the properties of materials rather than direct selection. For example, a number of natural structures such as honeycombs, coral colonies, arthropod eyes, and many echinoderm skeletons show a regular arrangement of hexagonal units. In the case of the honeycomb, individual bees are not genetically programmed to produce hexagonal cells in the beehive. An isolated bee would produce a circular cell; it is the simultaneous action of many individual bees, each one pushing outward as it constructs a single cell, that results in the geometrically close-packed structure. Similarly, comparison between the roughly circular perimeters of solitary corals and the hexagonal perimeters of the corallites of many colonial corals suggests a consequence of close packing.

Natural selection can only act upon the variation present in populations [SEE SECTION 3.1]. If there is no genetic variation for a trait, that trait cannot evolve, even if some modification would be advantageous to the organism. Thus, the absence of certain forms in the history of life need not imply that they would have been maladaptive. Likewise, some genetic variants may be generated by spontaneous mutation more often than others. The term **developmental constraint** is sometimes used to describe the nonrandomness of variation that results from the interaction between the genome and developmental processes. We saw in Chapter 4, for example, that the repeated evolution of byssal attachment in adult bivalve molluscs was probably facilitated by the presence of the byssus in the juvenile stage, a feature that could be retained by a simple modification of developmental timing. Thus, the variation on which selection can act is not strictly random. This reflects a combination of the historical and structural factors of Figure 5.1.

5.2 FUNCTIONAL MORPHOLOGY

The existence of a correlation between form and function is one of the oldest observations in biology. In some cases, the reason for the correlation may be at least partly phylogenetic. For example, living mammals that chew their cud have an even number of toes, but the number of toes clearly represents deep phylogenetic inheritance rather than an adaptation for digestion. In other cases, however, the form–function correlation clearly has an adaptive basis. Quadrupeds that run fast also have long limbs, for instance, and this can be understood from the mechanics of muscles and levers. The causal understanding of form–function correlation lies at the heart of functional morphology.

Given the assumption that adaptation is one of the main determinants of form, it is essential to identify those aspects of form that were the targets of selection in specific cases. Here we outline the basic ways in which function is inferred for extinct organisms, and we follow these with examples that illustrate the main approaches.

Throughout any functional analysis, it is essential to keep in mind that a structure may be involved in multiple functions. If these functions make conflicting demands on the structure, then not every function can be optimally performed. The result is a compromise, or **trade-off.**

Approaches to Functional Morphological Analysis

Inference from Homology The simplest way to infer function in extinct organisms is to consider homologous structures in living relatives. For example, we infer that most extinct birds used their wings to fly, unless the details of form suggest otherwise. Homology as a key to function is limited, because it is of no help in the many fossil species that have no close living relatives. It is also an inexact guide to function. *Archaeopteryx* and other primitive birds may have used their wings for flight. This does not imply that the style of flight was like that in any group of extant birds, however, for there has been extensive modification of the skeletal, muscular, and respiratory systems since the initial evolution of birds. Despite such limitations, evidence from homology remains an important component of many studies of functional morphology.

Inference from Analogy The function of skeletal structures may also be inferred from their close physical resemblance to convergent structures in distantly related species. This is what we do, for example, when we interpret the wings of pterosaurs as an apparatus for flight or gliding and when we interpret the streamlined form of ichthyosaurs as an adaptation for swimming. Because analogies can be inexact, analogous structures require thorough analysis before the precise details of their function can be understood.

Biomechanical Analysis Nearly all studies of functional morphology today involve **biomechanical analysis.** The function of problematic structures is deduced in light of the physical properties of biologic materials; mechanics of beams, levers, joints, and other structures; and aero- and hydrodynamics. Biomechanical analysis can be broadly categorized into two general approaches, the **paradigm approach** and the **experimental approach,** although the two are not completely distinct.

The concept of the paradigm in functional studies was introduced to paleontology in the 1960s by M. J. S. Rudwick, who was especially concerned with inferring function when homology and analogy could not be easily recognized. He defined the paradigm as "the structure that can fulfill the function with maximal efficiency under the limitations imposed by the nature of the materials" (Rudwick, 1961, p. 450). The paradigm approach typically involves three steps:

1. One or more potential functions are postulated for a problematic structure.
2. For each potential function, engineering principles are used to design the hypothetical structure optimally suited for carrying out that function. This structure is referred to as a *paradigm*. Because of trade-offs and limitations in the inherited body plan and materials, the optimal structures are not the best conceivable designs, but the best ones possible in light of these constraints.
3. The resemblance between the actual structure and the set of paradigms is assessed, and the paradigm that most closely resembles the actual structure is identified. The function corresponding to the closest paradigm is inferred to be the one that the actual structure most likely performed.

Assessing the resemblance between a paradigm and an actual structure involves some degree of subjectivity. For example, how closely must an elevated region on a bryozoan colony resemble a chimney for us to be confident that it indeed functioned, like a chimney, to facilitate fluid flow away from the colony surface? This uncertainty has contributed to a general preference for the experimental approach, which allows functional performance to be measured and verified. The experimental approach to biomechanics also involves three steps:

1. As with the paradigm approach, several potential functions are postulated for an unknown structure.
2. A model of the organism or structure is made. This model can be physical or numerical, and it can be highly simplified or a nearly exact replica.
3. The capacity of the structure to perform the function is assessed experimentally. Experimentation often involves manipulations such as removing a structure of interest from the model organism to determine whether its presence makes an appreciable difference to mechanical properties and function. For a simple physical or numerical model, there may be exact equations to determine its performance.

The paradigm approach and the experimental approach to biomechanical analysis share the advantage that they rely on universal physical laws and properties of materials. Both have the disadvantage of being limited by the range of postulated functions, and therefore by the imagination of the investigator. It is always possible that a structure may be best suited to a function that has not even been considered. Biomechanical analysis can only tell us whether an organism was capable of functioning in a specified way, not that it actually did so. Biomechanics has nonetheless been of great use in understanding the relationship between form and function in living as well as fossil organisms.

Examples of Biomechanical Analysis of Extinct Organisms

Vision in Trilobites The eyes of trilobites are similar in many regards to those of living arthropods. Therefore, much can be learned about the functional morphology of the trilobite eye by analogy with living forms. But there are important structural differences that suggest that the optical systems used by trilobites were significantly different. Much of our understanding of trilobite vision derives from an unusual collaboration between paleontologist Euan Clarkson and physicist Riccardo Levi-Setti. When the two met at a conference in Oslo in 1973, both had for several years been active students of trilobite morphology; Clarkson had done considerable work on trilobite vision, and Levi-Setti had a physicist's knowledge and understanding of optical systems.

Trilobites possessed a compound eye, consisting of numerous lenses arranged in rows (Figure 5.2). The lenses were usually deployed in a geometrically closely packed configuration. The lenses themselves were made of calcium carbonate in the form of the mineral calcite and are sometimes preserved. It has been possible experimentally to produce focused images through individual lenses. It is not known whether the animals could perceive a clear image, because this depends on

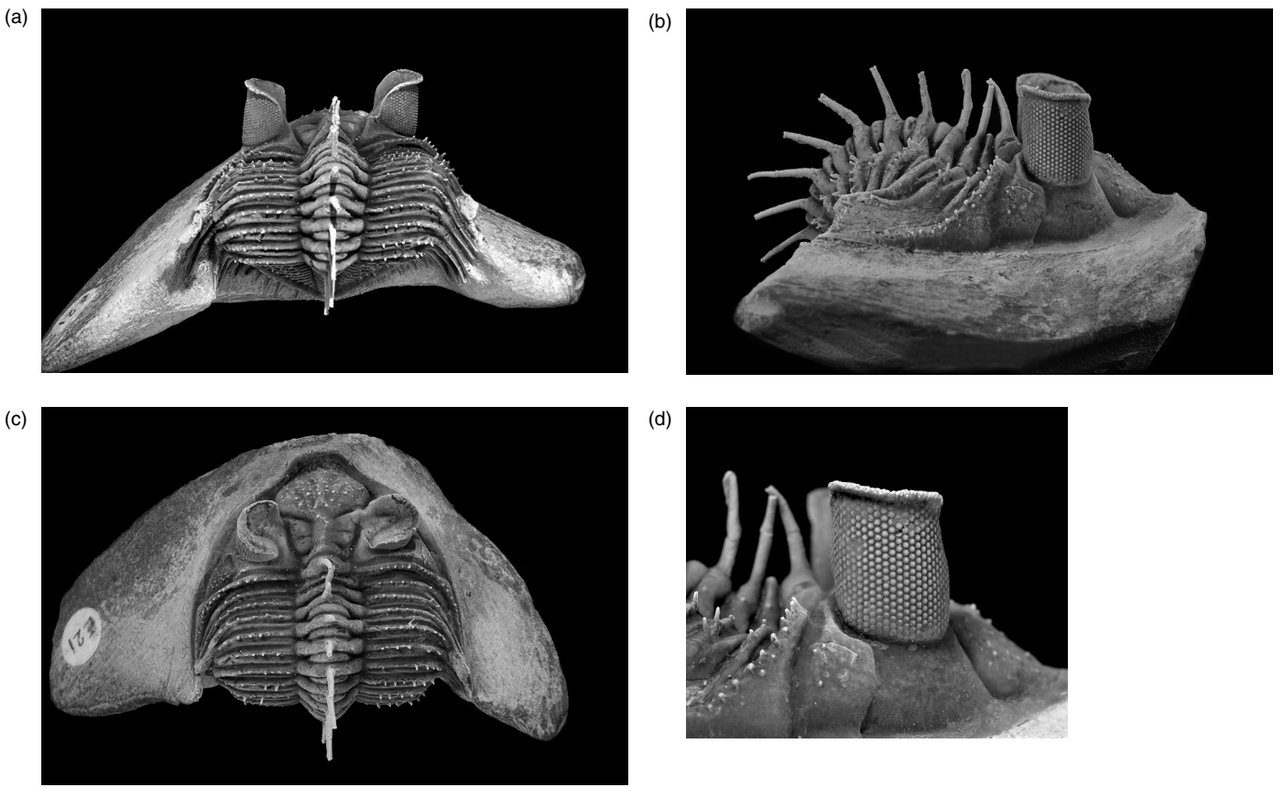

FIGURE 5.2 A trilobite with well-developed compound eyes, *Erbenochile* from the Lower Devonian of Morocco. (a–c) Posterior, lateral, and dorsal views. (d) Detail of eye, showing arrangement of individual lenses. Width of the head is 32 mm. *(From Fortey & Chatterton, 2003)*

the nervous system and unpreserved details of the eyes. But they could, at the very least, recognize movements of an object and estimate its size.

Lens morphology and the arrangement of lenses vary considerably from one group of trilobites to another. A particularly interesting lens shape is illustrated in Figure 5.3. It is a doublet consisting of an upper unit that is convex on its upper surface but has a more complex shape on its lower surface. Two variants of the shape of the lower surface are shown at the center in the illustration. In both variants, the lower part of the doublet has an upper surface that fits the shape of the upper lens and a lower surface that is simply convex. The two lenses together thus make a biconvex compound lens.

Upon examination of Clarkson's reconstruction of trilobite eyes, Levi-Setti noticed that the upper lenses just described are very close approximations of lens designs published by René Descartes and Christiaan Huygens in the seventeenth century. The Descartes and Huygens drawings are reproduced for comparison in Figure 5.3, left and right. The purpose of both designs was to produce what is known as an *aplanatic lens*—one that avoids certain kinds of distortion. The similarity between the shapes of the upper trilobite lens and the lenses designed by Descartes and Huygens is remarkable. Indeed, the lenses differ little, other than in the presence of the lower lens in the trilobite, an element that does not appear in the designs of either Descartes or Huygens. But this is understandable when it is noted that the aplanatic lens was designed to operate in air. Calculations have shown that in the trilobite's aqueous environment, the lower lens would be necessary to compensate for the relatively high refractive index of seawater. Thus, the trilobite lens doublet appears to be an optimal modification of basic designs that became a part of human technology only as recently as the seventeenth century. Similar correcting lenses have since been recognized in some living insects, ostracodes, and even scallops.

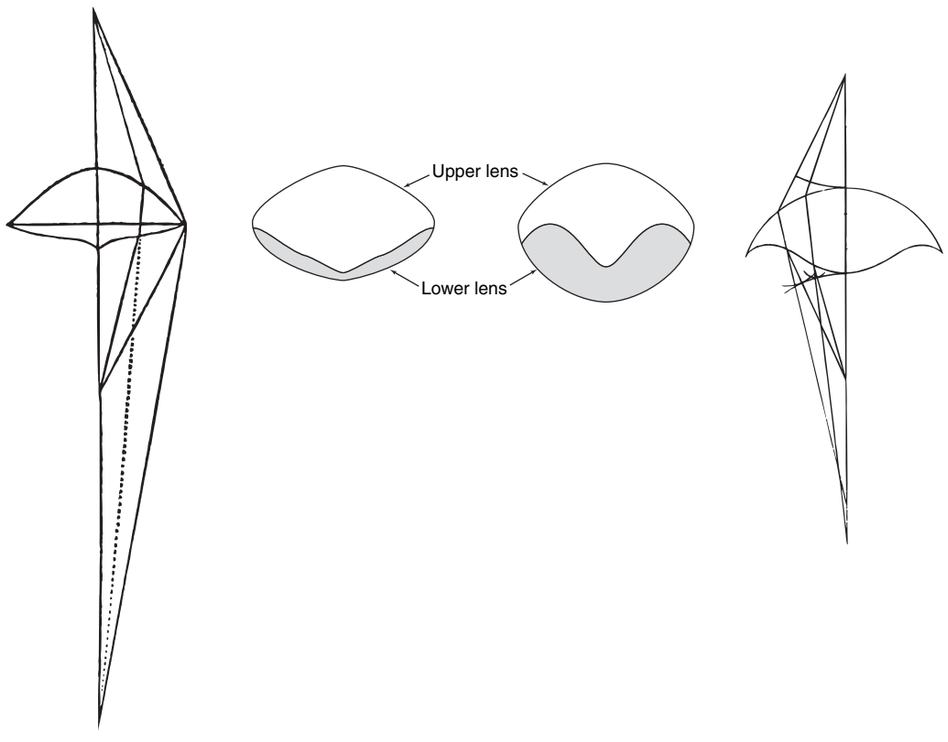

FIGURE 5.3 Lens morphology of two trilobites (*Dalmanitina socialis*, center left; *Crozonaspis struvei*, center right) compared with the original drawings for aplanatic lenses published by Descartes (left) and Huygens (right). Lenses are drawn in cross section; the vertical axis of each trilobite lens is normal to the surface of the compound eye. Both trilobites are of Ordovician age. *(Based on Clarkson & Levi-Setti, 1975)*

The trilobite lens is optimal in yet another way. Light was transmitted through the calcite lenses to photoreceptive cells within the eyes. The properties of calcite are such that light impinging on a crystal from virtually any angle is refracted in two directions, leading to a double image. However, if the crystal is oriented so that the light is moving parallel to its principal optical axis, the *c* axis (see Figure 2.14), the light will travel through the crystal as if it were glass. And this is precisely the orientation observed in trilobite lenses. The individual eye cells are oriented with respect to the curved eye surface in such a way that the *c* axes of the calcite lenses are normal to the eye surface.

To summarize, it appears from the work of Clarkson and Levi-Setti (1975) that trilobites evolved a remarkably sophisticated optical system. For an engineer to develop such a system would require considerable knowledge of optics and quite a bit of ingenuity. As an application of the paradigm approach to problems of functional morphology, the example provided by the trilobite lens is nearly unsurpassed.

As with many classic case studies that illustrate a principle unusually clearly, the interpretation of trilobite lenses has been scrutinized and challenged. First, it has been suggested that the doublet structure of Figure 5.3 may be a preservational artifact (Bruton & Haas, 2003). This possibility has not been completely evaluated, however, and the general consensus at the moment is that the trilobites in question had genuine lens doublets. Second, and more interestingly, some calculations have shown that the Descartes lens, which involved some mathematical approximations in its design, may not actually be well suited for minimizing spherical aberration (Gál et al., 2000). Yet some trilobite lenses have this shape. Why? Although we still do not know with certainty, some workers have suggested that the lenses may have functioned as bifocals, allowing focused images of near and far objects through different parts of the lens (Gál et al., 2000). We cannot predict how these questions will ultimately be resolved, but we can be sure that the function of trilobite eyes will continue to be a fascinating area of research.

Ventral Wing Plates in Crinoids Living stalked crinoids are erect suspension-feeders. They use their arms to capture suspended organic particles, which are then passed along an ambulacrum, or food groove, that runs the length of the arms toward the mouth, located centrally on the ventral side of the calyx (Figure 5.4). The feeding posture of living stalked crinoids is shown in Figure 5.5. The arms are recurved into the current, which flows from left to right in the photograph.

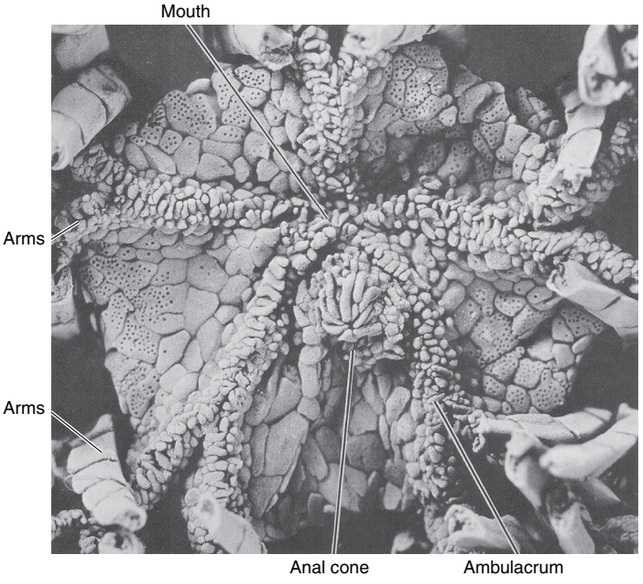

FIGURE 5.4 Ventral view of the living crinoid *Neocrinus decorus*, showing the central mouth, plated ambulacra, and bases of arms. Field of view is roughly 1 cm. *(From Moore & Teichert, 1978)*

FIGURE 5.5 Feeding posture of the living stalked crinoid *Cenocrinus*. The current flows from left to right, and the mouth is on the downstream side of the calyx. This crinoid is approximately 1 m tall. The photo was taken at between 200 and 300 m depth off the coast of Jamaica. *(Courtesy David L. Meyer)*

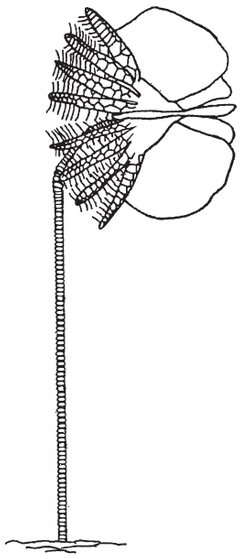

FIGURE 5.6 Reconstruction of the Early Carboniferous crinoid *Pterotocrinus depressus* in feeding posture. Posture is based on analogy to living stalked crinoids (Figure 5.5). The current flows from the left. Note the pronounced wing plates on the ventral side (facing to the right in this figure). *(From Baumiller & Plotnick, 1989)*

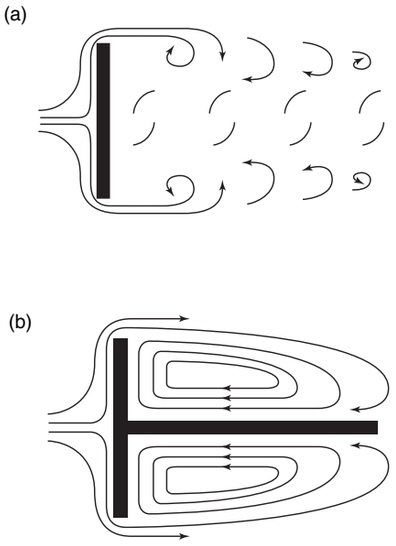

FIGURE 5.7 Splitter-plate effect, with flow from left to right. (a) Cross section of a blunt body in a flow; arrows indicate turbulent flow in the wake. The separation of flow induces a low-pressure region in the wake and thus increases drag. (b) Similar body with a splitter plate; arrows indicate laminar flow. Separation of flow is delayed and drag is reduced. *(From Baumiller & Plotnick, 1989)*

The current goes around the arms and through the openings between arms, and the food particles are captured on the downstream side of the arms. By homology, most extinct stalked crinoids are thought to have functioned in the same way.

Certain Carboniferous crinoids, most notably the genus *Pterotocrinus*, are unusual in possessing large, wing-like plates that protrude from the ventral surface of the calyx (Figure 5.6). In an experimental study of *Pterotocrinus*, Tomasz Baumiller and Roy Plotnick (1989) postulated two potential functions for the wing plates.

First, they may have served as "splitter plates." It is well known from hydrodynamics that the flow around a blunt body separates, producing a low-pressure region in the wake and increasing drag on the body (Figure 5.7a). Adding a long plate to the object in the downstream direction helps to reduce drag by delaying the separation of flow, thus reducing the diameter of the wake (Figure 5.7b). Drag reduction could be beneficial to the crinoid by enabling it to maintain the appropriate feeding posture and by reducing stress on the ligaments of the stalk.

Second, the plates may have served as rudders, enabling the crinoid to maintain its feeding posture by reorienting passively when the current direction changed, much as the tail of a weather vane keeps it pointed into the wind.

To explore these two possibilities, Baumiller and Plotnick constructed an idealized physical model of a crinoid feeding apparatus: a fine steel screen formed into a hemispherical bowl (Figure 5.8). This model crinoid was attached via rigid rods to ball bearings so that the model could turn, and the apparatus was attached to a strain gauge so that the forces on the model could be measured. Experiments were conducted by placing the model in a flume—the hydrodynamic equivalent of a wind tunnel—and varying the speed of the current and its direction relative to the models. Models with and without wing plates were tested. To ensure that results did not depend critically on the particular experimental conditions, the experiments spanned a wide range in current speed; the angle between the current and the model; the coarseness of the wire mesh; and other aspects of the model, such as the distance between the ball-bearing pivot and the "calyx." Current speeds were also kept within a biologically realistic range.

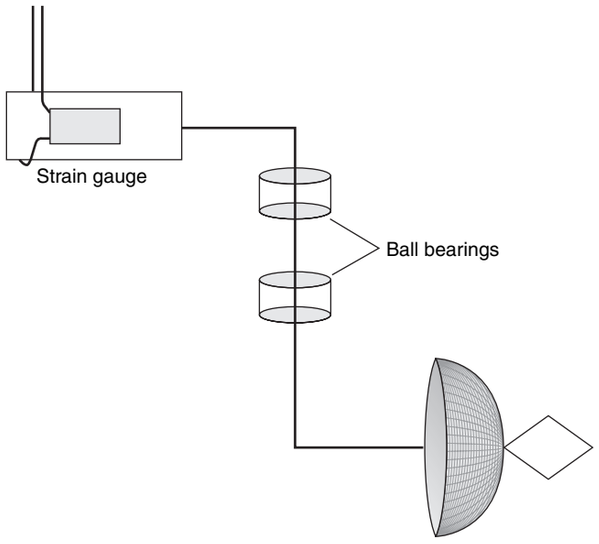

FIGURE 5.8 Experimental design for measuring forces on crinoid models. The wire-mesh hemisphere simulates the crinoid in feeding posture, and the diamond-shaped plate simulates the wing plate. Ball bearings allow the model to swivel passively, and the strain gauge measures the forces on the model. The current flows from left to right. *(From Baumiller & Plotnick, 1989)*

To test the hypothesis that the wing plates in *Pterotocrinus* may have functioned as splitter plates, the drag force on models with plates was compared with the force on models without plates. Models were oriented with the concave side of the wire-mesh hemisphere pointing upstream, consistent with the feeding posture of living crinoids. The splitter-plate hypothesis predicts that models with plates should experience lower drag forces. In fact, the drag forces on the two models were found to be indistinguishable (Figure 5.9a). This suggests that the wing plates were unlikely to have functioned to reduce drag.

To test the rudder hypothesis, the models were turned away from the concave-upstream posture by specified angles. If the wing plates functioned effectively as rudders, then the models with plates should experience greater rotational forces than the models without plates. This is exactly what happened (Figure 5.9b)—which suggests that the rudder hypothesis is plausible; crinoids with wing plates could have used them to reorient themselves passively.

In summary, a simplified but hydrodynamically relevant model of an erect crinoid shows that specialized structures—the wing plates—probably did not function to reduce drag but may well have enabled crinoids to maintain the proper feeding posture without expending energy to turn into the current. This represents an exemplary case of the use and experimental manipulation of physical models, combined with knowledge of living representatives, to deduce the function of extinct organisms. The next example illustrates these same themes, but differs in using replicas of actual specimens.

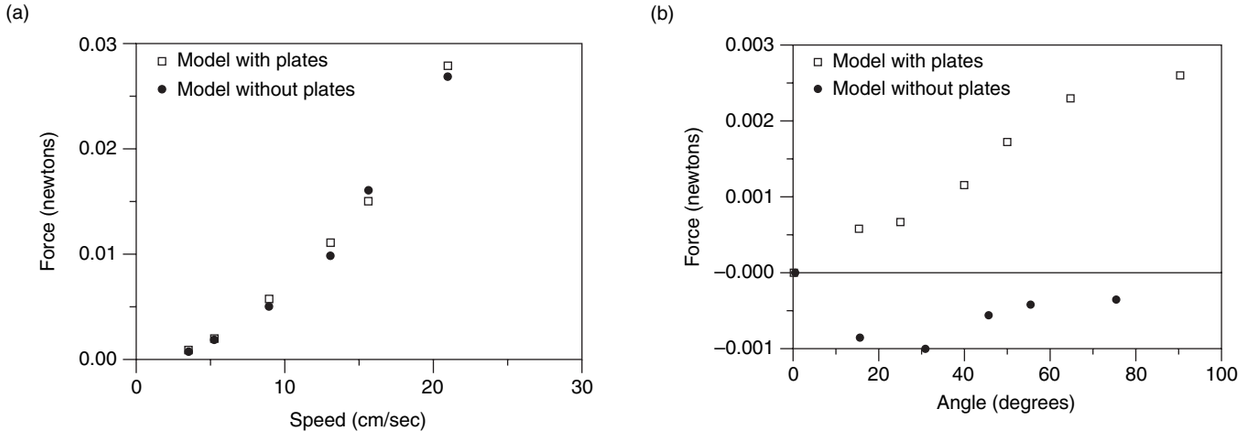

FIGURE 5.9 Results of experiments on crinoid models of Figure 5.8. (a) Drag force on the models versus current speed. There is essentially no difference in drag between models with and without wing plates. (b) Rotational force on the model versus angle between the model and the current. Forces with a positive sign are those that cause the wire-mesh bowl to turn into the current. The models with plates are able to reorient passively into the current, whereas the models without plates are not. *(From Baumiller & Plotnick, 1989)*

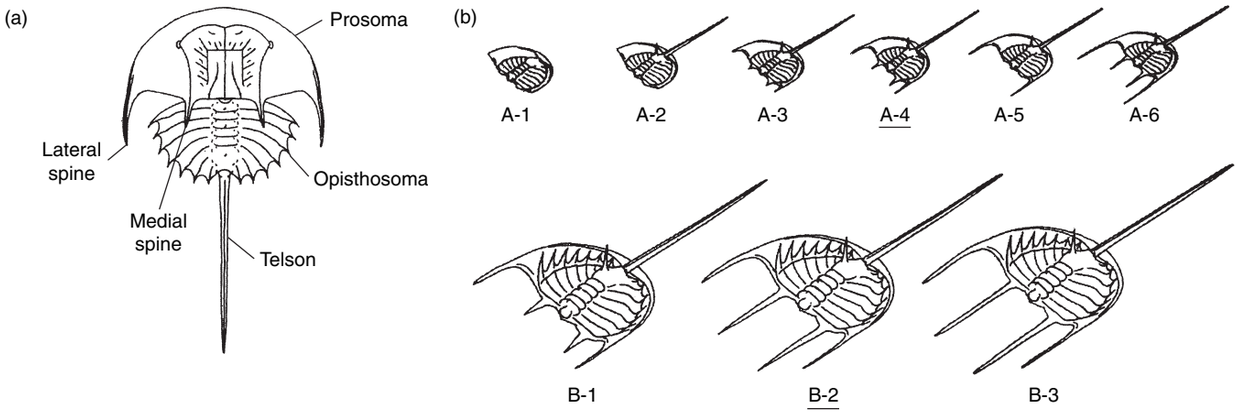

FIGURE 5.10 Late Carboniferous horseshoe crab *Euproops danae*. (a) Reconstruction. (b) Fabricated models. Models are in an enrolled posture, with the posterior tucked up under the anterior and the telson projecting forward. The A and B models are juveniles and adults. A-4 and B-2 are actual forms; the others have had the spines artificially lengthened or shortened. *(From Fisher, 1977)*

Spines in Horseshoe Crabs Spines and other projections are common in a wide range of organisms. Their function is often regarded, quite reasonably, as protective. The adaptive value of the precise morphological details of spines—their size and shape—is usually less clear, however. *Euproops*, a Late Carboniferous arthropod related to living horseshoe crabs, possessed two pairs of spines on the anterior body region, or prosoma (Figure 5.10). One intriguing property of these spines is that, in juveniles, the lateral pair is longer than the medial pair. The medial spines grow faster, however, so in adults they are longer than the lateral spines. The function of spines was explored experimentally by Daniel Fisher (1977), who considered both the general role of spines and the reason for their relative sizes.

Living horseshoe crabs are known to burrow for protection. Because previous functional studies had shown that *Euproops* was probably a capable swimmer, Fisher reasoned that individuals were likely to encounter predators well above the substrate, where burrowing would not be an option. Numerous arthropods, living and extinct, are known to enroll, evidently in response to disturbance. There is anatomical evidence that *Euproops* was capable of enrollment—such as the fit in shape between the prosoma and rear body region, or opisthosoma. Moreover, specimens are commonly preserved in an enrolled position.

If an individual enrolled upon encountering a predator, it would settle toward the substrate and potentially escape predation. The predators of *Euproops* would have included fishes and amphibians with basic sensory systems similar to those of living forms. Observations of many modern fishes demonstrate that they are highly sensitive to horizontal motion in their prey. A smooth path of settling would therefore make the horseshoe crab less conspicuous to a predator than would an oscillatory or irregular path in which horizontal movements interrupt the general vertical descent.

Given this background, Fisher explored the role of spines in settling. He constructed models of horseshoe crabs, allowed the models to fall freely in sea water, and filmed their settling behavior. Figure 5.10b shows two sets of models, one of juveniles (A) and one of adults (B). For each set, one model has spines with realistic lengths while the other models have spines that have been made longer or shorter compared with real forms or have had their relative lengths changed. The models are reconstructed in an enrolled posture, with the opisthosoma tucked under the prosoma and the telson (tail spine) extending beyond the head.

Representative results of settling experiments are shown in Figure 5.11. Some of the models oscillate as they descend (A-6), others make abrupt horizontal shifts (A-2), and some attain a smooth and stable descent (A-4). This last type of settling is expected to be least conspicuous to a predator, and therefore to be most advantageous for predator avoidance. The models that settle in this way are in fact the ones corresponding to the observed forms. For juveniles, relatively long lateral spines and relatively short medial spines, both of

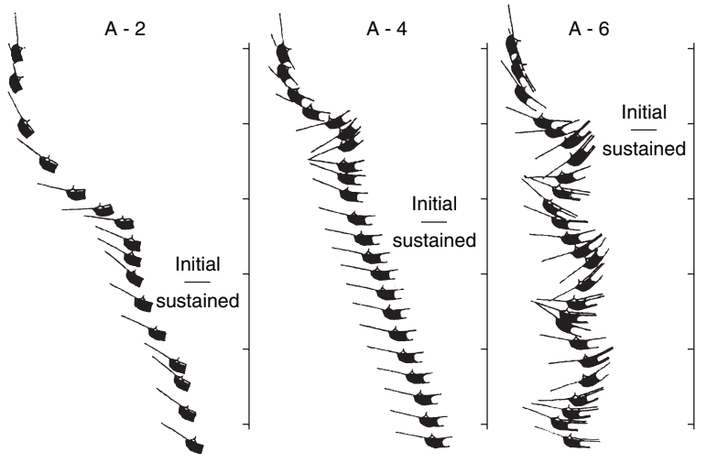

FIGURE 5.11 Examples of settling behavior of juvenile *Euproops* models, drawn from time-lapse photographs. Models were released in water with tail spine pointing up. They initially moved from this orientation, then achieved a sustained pattern of descent. A-4 shows the steady descent of a realistic form. A-2 and A-6 show examples of unsteady descent in forms that have had spines changed from their true lengths. *(From Fisher, 1977)*

Box 5.1

LOCOMOTION IN NONAVIAN DINOSAURS

In any long-lived and diverse biologic group, it is unlikely that any aspect of function will be completely uniform throughout the group. Nevertheless, it may be possible to characterize the general functional style of a higher taxon and to contrast it with that of other taxa. The case of dinosaurs is especially interesting because there is a living group that is phylogenetically close to them—the birds, which are generally recognized to be an offshoot of theropod dinosaurs.

Despite their evolutionary descent from dinosaurs, living birds are highly derived in terms of physiology, behavior, feeding, and skeletal anatomy. Basal phylogenetic relationships within archosaurs (Figure 4.10) might also seem to suggest crocodilians as a possible living analog for some dinosaurs. At the same time, the wide range of ways of life apparently exploited by dinosaurs as a group, many of them similar to those of living mammals, suggest the possibility of mammals as living analogs. The following study focuses on a particular aspect of function—namely, the posture adopted in walking—to determine which living group is likely to represent the best analog.

Many aspects of skeletal morphology in dinosaurs suggest an upright posture, so the sprawling gait of crocodiles and other primitive archosaurs would seem to be ruled out. Yet within this upright posture, there are two principal styles of locomotion, broadly characteristic of birds and of mammals, respectively (Figures 5.12 and 5.13). The orientation of the femur changes throughout the step cycle in both groups, generally being relatively more vertical at the point of foot lift-off and more horizontal at the point of foot contact (Figure 5.13). The forces on the femur also vary regularly with the step cycle, being dominated by torsion and compression when the femur is horizontal, and bending and compression when it is vertical (Figure 5.12d and 5.12e). Regardless of the point in the step cycle, however, birds tend to have the femur at a position much closer to horizontal than do mammals (Figure 5.13).

The relatively horizontal posture of the femur has important consequences for avian skeletal structure. Consider the total length of the hindlimb and the proportion of this length made up by the femur, the tibia, and the metatarsal (Figures 5.14 and 5.15). The femur of a bird typically accounts for 20 to 40 percent of the total limb length. Bone is weaker in the face of torsional as opposed to bending forces. This, coupled with the horizontal attitude of the bird femur, implies that the torsional forces on this bone would be excessive if it were much longer than 40 percent of the limb length. With a more vertical femur, mammals experience a lower torsional force and can therefore achieve longer femoral lengths, up to 60 percent or more of the total limb length.

which are short relative to the prosoma, are required to yield a smooth descent. For adult models to settle smoothly, spines must be about the same length as the prosoma. Fisher found that and the medial spines must be longer than the lateral spines. This again is what is seen in actual specimens. These results strongly suggest that the right balance of spine sizes is an adaptation for smooth settling. Because there are nonlinear relationships between spine size and body size on the one hand and drag and other hydrodynamic forces on the other hand, the same spine sizes are not equally effective at all body sizes. There has evidently been natural selection for a particular pattern of anisometric growth [SEE SECTION 2.3] in order to accommodate this fact.

Although the spines of *Euproops* clearly have functional value, the settling behavior of this horseshoe crab is not perfectly ideal. Rapid, smooth settling would be better attained by a spherical object. Yet the organism had functional demands other than settling. For example, its overall form was elongate rather than spherical in order to facilitate swimming, and the spines projected posteriorly to facilitate movement through the sediment. *Euproops* could settle remarkably smoothly; it is as optimal as can reasonably be expected, given the constraints of competing functions and phylogenetic inheritance (Figure 5.1).

The additional example in Box 5.1 combines biomechanics with statistical analysis of anatomical measurements.

Thus, we have a form–function correlation that can be understood in terms of biomechanics. Can we use this to deduce the style of dinosaur locomotion? The argument for doing so is statistical in nature. When dinosaur limbs are measured, they largely overlap the mammalian field in the

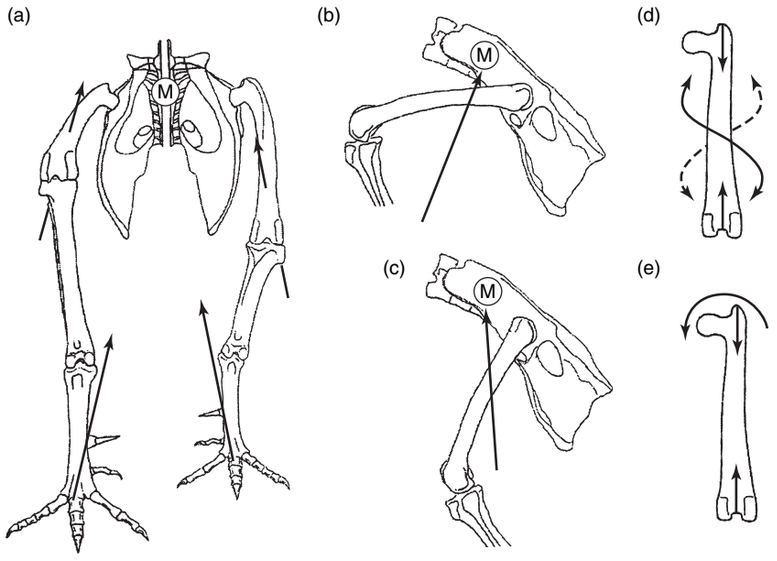

FIGURE 5.12 Posture and biomechanics of a representative terrestrial vertebrate (a chicken). (a) The pelvis and hindlimbs. The lower arrows indicate the direction of force between the ground and the center of mass, M. The upper arrows indicate forces through the femur that result from the offset between the femur and the center of mass. (b, c) Two parts of the stride in which the femur is (b) relatively more horizontal and (c) more vertical. (d, e) The forces on the femur, indicated diagramatically. When the femur is more horizontal (d), there are compressive forces (straight arrows) and twisting forces (curved arrows). When the femur is more vertical (e), there are compressive forces (straight arrows) and bending forces (curved arrow). *(From Carrano, 1998a)*

continued on next page

Other Lines of Evidence in Functional Interpretation

Numerous other lines of supplementary evidence are often invoked in functional studies. As discussed in Chapter 1, trace fossils may reveal patterns of behavior that give clues to function and aspects of life habit. Studies of growth are also important in functional analysis. In the example of respiration in rhombiferan echinoderms that we discussed in Chapter 2 (Box 2.3), the details of allometric scaling were used to infer that some factor must have limited the efficiency of respiratory structures. In the example that follows, additional geologic and paleogeographic data are used to help infer the functional ecology of certain specialized trilobites.

Life Habits in Pelagic Trilobites The range of individual lens orientations in the trilobite eye can be used to infer the size and shape of the visual field of the trilobite. In most trilobites, the field of view is lateral, over the surface of the sediment. A number of trilobite lineages independently evolved large eyes that, in the most extreme cases, gave them 360° vision in all directions, including downward (Figure 5.16). The specialized eyes of the forms in Figure 5.16 are accompanied by other unusual features that are not generally found in trilobites, the majority of which

Box 5.1 (continued)

femur–tibia–metatarsal ternary diagram (Figure 5.15), while they show only slight overlap with the avian field. Note that the oldest known bird, *Archaeopteryx*, falls within this small region of overlap. Bipedal and quadrupedal dinosaurs occupy nearly separate fields, but both are mainly coincident with the mammalian field.

Overall, the structure of dinosaur limbs suggests a style of locomotion more similar to that of living mammals than to that of living birds. This result, of course, does not mean that other aspects of dinosaur function and physiology are more mammalian than avian, but it is important in providing an analog for future studies of dinosaur locomotion.

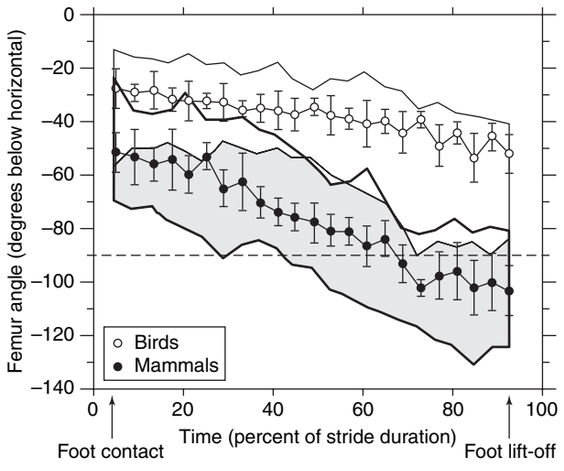

FIGURE 5.13 Posture of the femur during the stride of birds (open circles) and mammals (closed circles). The angle of the femur relative to the horizontal varies predictably during the stride, and this angle is consistently lower (more horizontal) for birds. Points show the mean ±1 standard error (see Box 3.1), based on four bird species and eight mammal species. *(From Carrano, 1998a)*

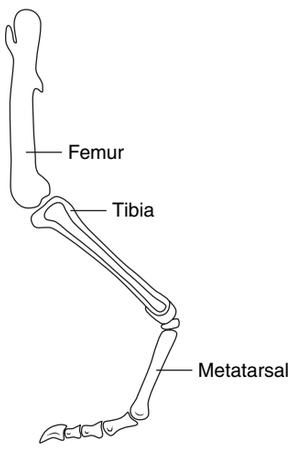

FIGURE 5.14 Sketch of a hindlimb showing femur, tibia, and metatarsal that were measured for comparison among birds, mammals, and dinosaurs. *(From Carrano, 1998b)*

were benthic (bottom-dwelling) and had the ability to walk and swim to a limited extent. The pleural (lateral) regions of the thorax in these specialized forms are greatly reduced, which would have contributed to flexibility and reduced the bulk of the trilobite. This would seem to serve as an adaptation for swimming. The reduction in pleural regions may also have facilitated backward vision.

The head is large and has genal spines that project downward. This is different from the majority of trilobites, whose spines project horizontally, and it would not have been conducive to a benthic existence. Moreover, the axial region is highly vaulted, suggesting well-developed musculature, like that of a shrimp, that would have been useful for active swimming. This combination of features suggests that these trilobites were pelagic (open-ocean) rather than benthic.

The well-developed eyes are similar to those seen in a number of specialized living species of amphipod and isopod crustaceans. These groups are mostly benthic, but specialized forms that live in the open ocean have evolved large eyes like those of the trilobites in question. By analogy, this suggests that these trilobites were also pelagic. As stated earlier, arguments from analogy can be rather inexact. But in this example, there are two additional lines of evidence that support the inferences drawn from functional arguments and analogy.

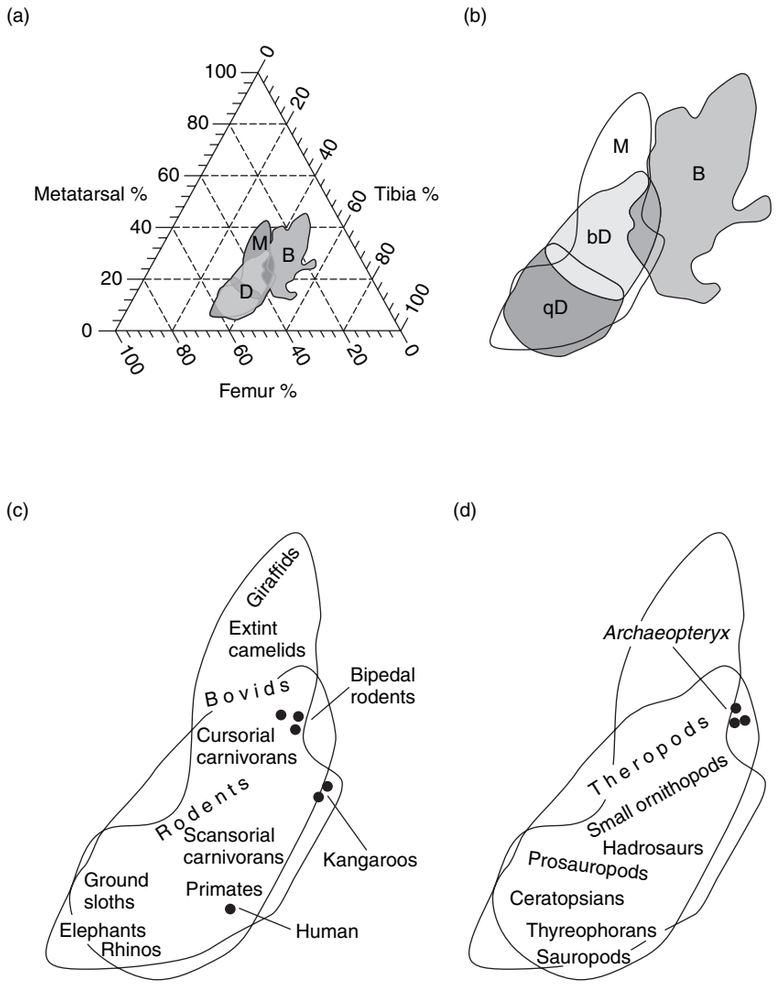

FIGURE 5.15 Hindlimb measurements for birds (B), mammals (M), and nonavian dinosaurs (D). (a) The percent of the total hindlimb length accounted for by the femur, tibia, and metatarsal is graphed in the ternary diagram. Lines circumscribe the entire field of values for each group. (b) Details of the fields occupied by the three groups. Bipedal dinosaurs (bD) overlap somewhat with birds, but both bipedal and quadrupedal (qD) dinosaurs overlap mainly with mammals. (c) The positions of some groups of mammals. Note that bipedal mammals (indicated by the dots) largely overlap with the field of bipedal dinosaurs. (d) The positions of some groups of dinosaurs. Note that three specimens of the oldest known bird *Archaeopteryx* are within the field of bipedal dinosaurs. *(From Carrano, 1998a)*

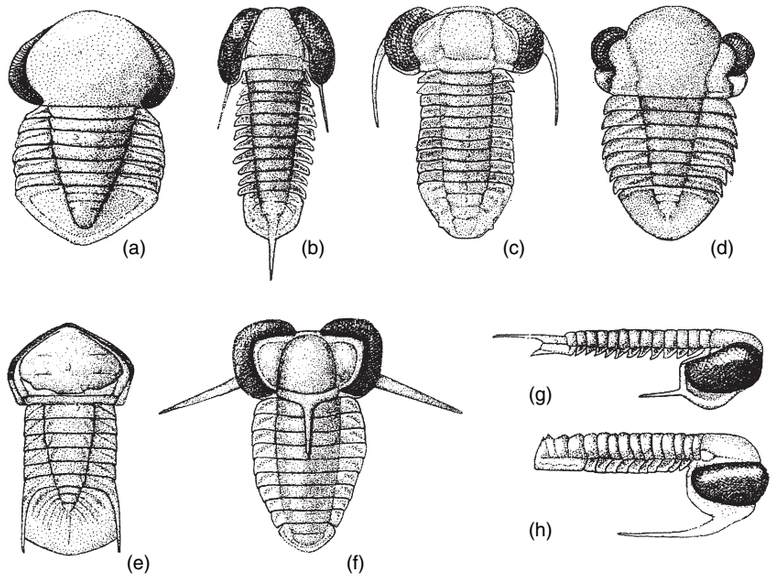

FIGURE 5.16 Examples of trilobites with well-developed eyes, reduced pleural regions, and ventrally projecting heads. (a–f) Dorsal views of *Pricyclopyge*, *Opipeuterella*, *Carolinites*, *Prospectatrix*, *Girvanopyge*, and *Telephina*. (g, h) Lateral views of *Opipeuterella* (b) and *Carolinites* (c). *(From Fortey, 1985a)*

First, individual taxa of these trilobites have very broad geographic ranges but are mostly restricted to near the paleoequator (Figure 5.17). This suggests that ocean conditions rather than dispersal ability and the arrangement of continents [SEE SECTION 9.6] limited their distribution. Second, the trilobites are found in a wide range of sediment types, ranging from the kind of shallow-water deposits in which benthic trilobites are usually found to deeper water sediments. It seems implausible that a species would occupy such a wide range of benthic environments without showing any anatomical modifications to suit the different habitats. In fact, other lineages of trilobites that live on the sediment surface in very deep waters, where little light penetrates, often have reduced or absent eyes.

The natural interpretation of this combination of geographic and geologic occurrence is that these trilobites, like the amphipods and isopods mentioned earlier, lived in the open ocean and that their molts and carcasses settled to the ocean floor to occupy a range of sedimentary environments. Further refinement of this interpretation is possible. Different genera of pelagic trilobites are found in a somewhat different range of sediment types. Molts and carcasses settled to the ocean floor, and the shallower the pelagic habitat of the taxon, the broader the range of depths to which it could settle (Figure 5.18).

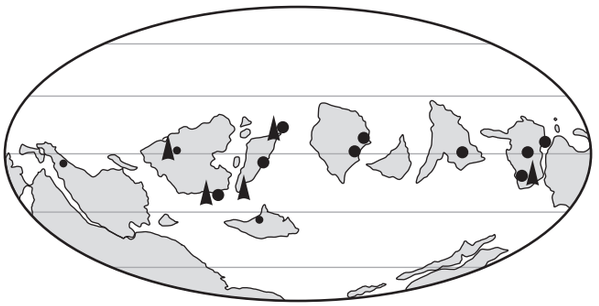

FIGURE 5.17 Paleogeographic reconstruction showing the arrangement of continents in the Early Ordovician. Circles show occurrences of the genus *Carolinites* (Figures 5.16c and 5.16h), and triangles show occurrences of *Opipeuterella* (Figures 5.16b and 5.16g). Both are geographically widespread but mostly near the paleoequator, suggesting that they were limited by ocean conditions rather than dispersal ability. *(From Fortey, 1985a)*

Genera such as *Carolinites* (Figures 5.16c and 5.16h) and *Opipeuterella* (Figures 5.16b and 5.16g), which are found in the full range of environments from shallowest to deepest, must have inhabited the surface waters. Others, such as *Pricyclopyge* (Figure 5.16a) and *Girvanopyge* (Figure 5.16e), which are absent from the shallowest sediments, must have lived within the deeper parts of the ocean.

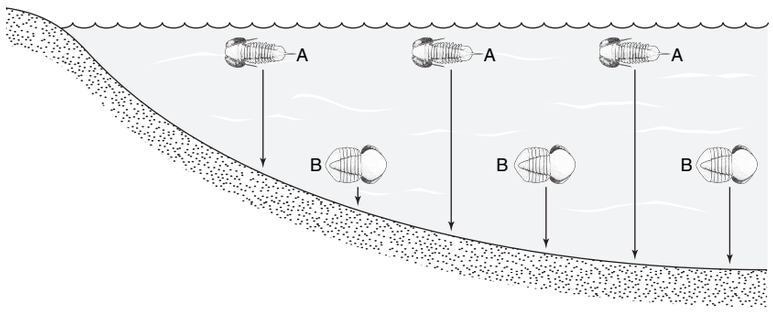

FIGURE 5.18 The distribution of sedimentary environments in which pelagic trilobites are found depends on the depth at which they lived. Arrows indicate settling to the sea floor after death or molting. A surface-dwelling form (A) can be found in sediments representing a wider range of water depths, whereas a form that lives at depth (B) will be absent from deposits representing shallower water. *(Based on Fortey, 1985a)*

5.3 THEORETICAL MORPHOLOGY

The foregoing examples of functional morphologic analysis illustrate adaptation and trade-offs in individual organisms and structures. These same factors are important in shaping the distribution of form within larger biologic groups. If some aspect of form is highly adaptive, we should expect it to be quite common, subject to the limitations imposed by history, structure, and competing functional demands.

There are generally three main features in a study of theoretical morphology: (1) A formal model of morphology is set forth [SEE SECTION 2.2]; (2) this model is used to generate the spectrum of possible forms that adhere to the assumptions of the model; (3) the distribution of known forms is compared with the theoretically possible spectrum. Differences between the possible and the actual, such as preferred modes and gaps in the actual distribution, are explored using functional morphology and other lines of reasoning.

In the sections that follow, we outline some major themes of research in theoretical morphology, illustrating each with a different model of form. Certain models, such as the harmonic analysis of curves (see Box 2.2), involve a large number of parameters and are therefore of limited practical use in exploring the relationship between conceivable and actual distributions of form. For our purposes, it is convenient to restrict discussion of theoretical morphology to models with relatively few parameters.

Exploring Alternative Modes of Life

Geometric Analysis of Shell Coiling A wide range of organisms produce coiled skeletons and skeletal parts that are mathematically well characterized. The growth of mollusc and brachiopod shells, for example, can be modeled as the movement of a generating curve around an axis of coiling, sweeping out a three-dimensional solid of revolution (Figure 5.19). The generating curve may approximate the aperture or opening of the shell, but the generating curve and coiling axis are mathematical constructs rather than biological structures.

The generating curve changes in size as it revolves about the axis. The whorl expansion rate W expresses this change in size as the ratio of sizes of the generating curve separated by a full revolution, or 2π radians (360°). Because we are concerned with biological traits, which

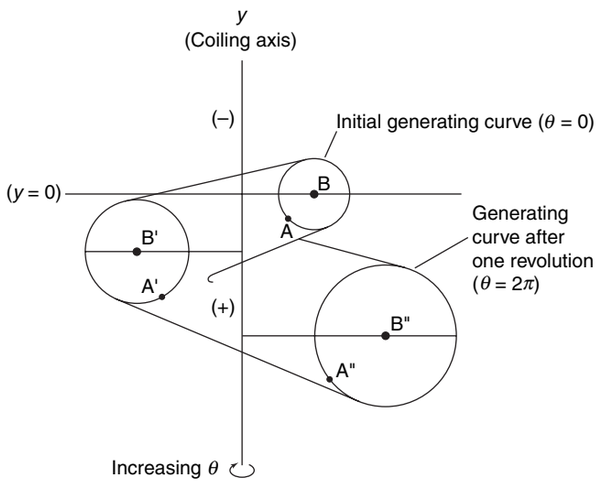

FIGURE 5.19 Geometric model of shell coiling, depicted in cylindrical coordinates. The movement of the generating curve about the coiling axis sweeps out a three-dimensional solid of revolution. Θ gives the angular revolution of the generating curve about the coiling axis, and y represents the distance along the coiling axis. A, A′, and A″ represent a point on the generating curve at 0, π, and 2π radians of revolution. B, B′, and B″ represent the center of the generating curve. *(From Raup, 1966)*

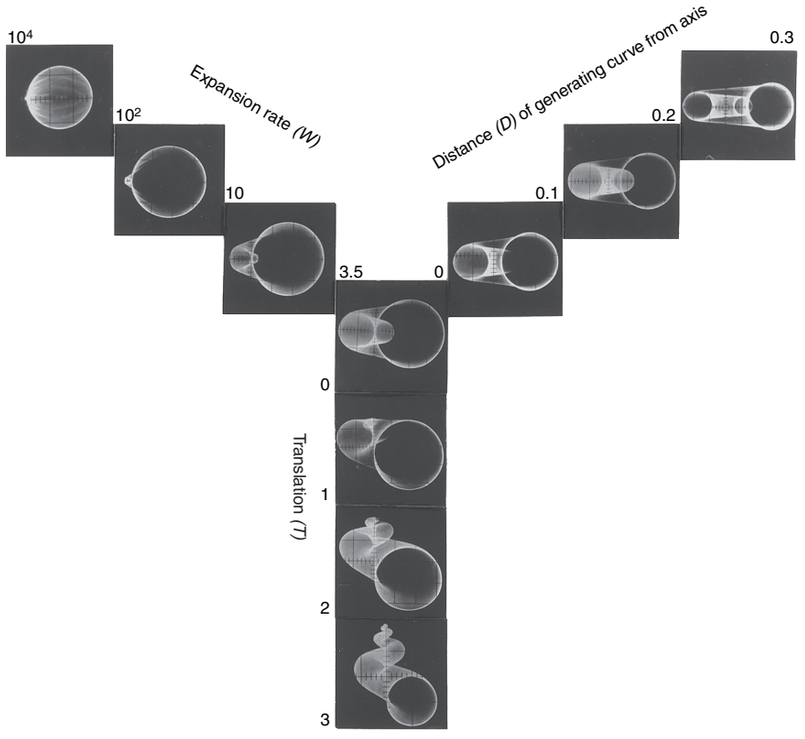

FIGURE 5.20 Some hypothetical shells generated by computer using the model of Figure 5.19. This figure shows the effect of varying each of the three parameters of the coiling model while keeping the others constant at the values indicated for the shell in the center. *(From Raup, 1966)*

generally increase in size as the organism grows, the theoretical lower limit on W is 1. W has no theoretical upper limit.

The generating curve may also move along the axis as it revolves and expands. The rate at which it does so is the translation rate T, expressed as a ratio of how far along the y axis a point on the generating curve moves relative to how far away from the y axis it moves. If T is equal to zero, the shell coils in a plane (Figure 5.20, center), as is the case for most cephalopods. The model shell in Figure 5.19 is dextral; that is, it turns in the sense of a right-hand screw. For reasons that are still not fully understood, the vast majority of gastropods that have ever lived are dextral. For dextral shells, T is positive—that is, the curve translates down the axis. For sinistral or left-hand shells, T is negative and the curve translates up the axis. In either case, the magnitude of T has no theoretical upper limit. All else being equal, the higher the translation rate, the greater the height-to-width ratio of the shell (Figure 5.20, bottom series).

The final parameter of the coiling model is the relative distance D of the generating curve from the coiling axis. This is defined as the distance from the coiling axis to the inner margin of the generating curve, divided by the distance to the outer margin. The generating curve is assumed not to overlap the axis of coiling; thus $D \geq 0$. If the generating curve just touches the coiling axis, then $D = 0$. Distance D has no theoretical upper limit.

From the definition of W, it is clear that this geometric model assumes multiplicative growth in size. If the coiling parameters are constant, the shape of the shell remains constant as size increases. Figure 5.20 shows a range of coiled shells that can be simulated with this simple model. In many ways, they succeed in mimicking real shells, although they also fail in some respects. For example, it is common for molluscs and other coiled organisms to change their coiling geometry as they grow, sometimes gradually and sometimes abruptly, as at the transition from larva to juvenile (see Figure 7.29), but this is not taken into account in the simple model of Figure 5.19. Also, the generating curve is assumed to be circular for simplicity, while the cross sections of real whorls vary enormously in shape.

Ontogenetic changes in coiling parameters could be incorporated into the model, and the shape of the generating curve could itself be modeled with one or more parameters to make the resulting forms more

realistic. However, the goal of morphological modeling is generally not to produce exact replicas of organisms. To do so would involve a complex description with so many parameters as to make the model practically useless.

The model tells us how to simulate ideal shells. If we are to compare these with actual forms, it is necessary to estimate the coiling parameters from real shells. One way to do this is described in Box 5.2. Analogous operational procedures must be devised for other models considered later in this chapter. Although mathematical models of form may seem highly abstract, it is often easier to work with models than to measure actual specimens!

Box 5.2

ESTIMATING COILING PARAMETERS

To calculate the values of W, T, and D for a coiled shell, it is necessary to estimate the position of the coiling axis and to identify the generating curve. This is commonly done by cutting a cross section of the shell or by taking an X-ray.

Figure 5.21a shows the adult shell of the extant land snail *Theba pisana*. A radiograph of another specimen of this species, printed as a negative, is shown in Figure 5.21b. This simulates sectioning of the shell without actually damaging it [SEE SECTION 2.2]. Here we can make out the outline of the coiled tube at successive whorls. These outlines are assumed to represent the ideal generating curve.

A line drawing of the generating curve at increments of π radians is shown in Figure 5.21c. Superimposed on these is an estimate of the position of the coiling axis. In this case, the coiling axis was fitted by eye, but more exact statistical approaches can be used to find the optimal position of the axis.

Assuming the shell fits the coiling model, D can be estimated from the generating curve at any point, and W and T can be estimated from the generating curve

(a)

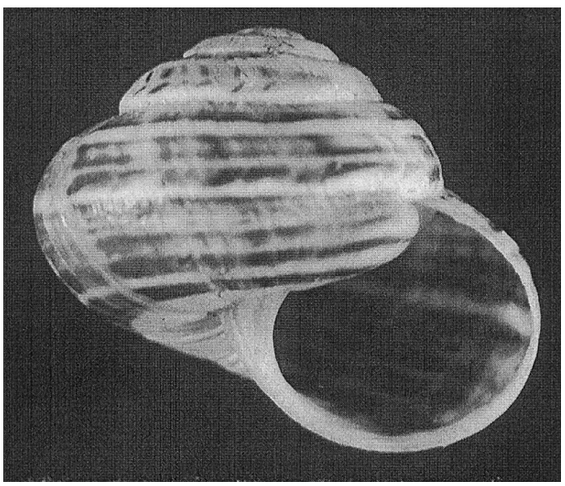

(b)

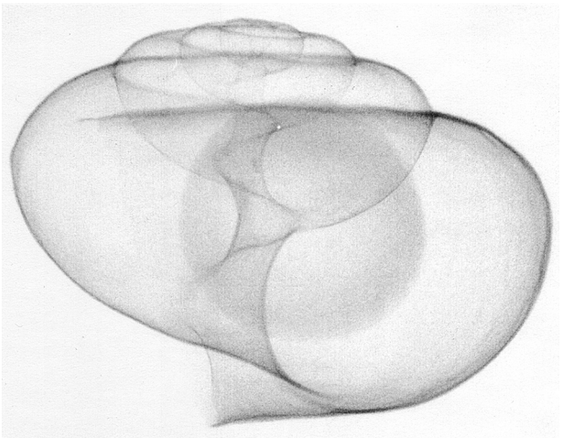

FIGURE 5.21 Estimation of coiling parameters. (a) Photograph of the living land snail *Theba pisana*. The width of the shell is about 1.5 cm. (b) Enlarged radiograph of a shell, printed as a negative, used to obtain the image of the cross section. The large, subcircular feature near the center of the image is a ball of plasticene used to hold the shell in place for radiography. *(Michael Foote)*

continued on next page

Box 5.2 (continued)

at any two points separated by 2π radians, as shown in Figure 5.21c. Here D is calculated as d_{in}/d_{out} on the final whorl. The heavy points show the position of the geometric centroid of the generating curve. The x- and y-coordinates of these points are used to calculate W and T, as follows:

$$W = x_{\Theta+2\pi}/x_{\Theta}$$

and

$$T = (y_{\Theta+2\pi} - y_{\Theta})/(x_{\Theta+2\pi} - x_{\Theta})$$

That these expressions are appropriate can be verified by comparing them with the model in Figure 5.19. Other approaches are also commonly used. For example, if A is the measured area of the generating curve, W can be calculated as $\sqrt{(A_{\Theta+2\pi}/A_{\Theta})}$. The square root is taken because W is defined as the rate of increase of a linear feature.

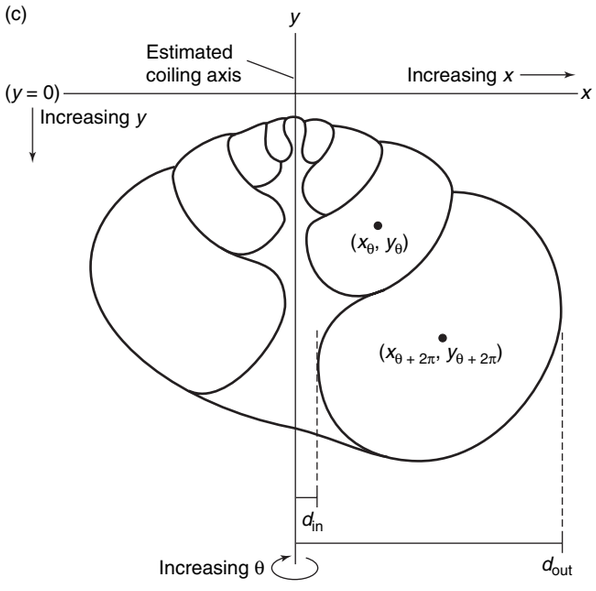

FIGURE 5.21 (*cont.*) (c) Line drawing of the whorl outlines from the radiograph, used to estimate the position and size of the generating curve. The vertical line is the estimated coiling axis. Heavy points denote the geometric centroid of the generating curve. $D = d_{in}/d_{out}$, $W = x_{\Theta+2\pi}/x_{\Theta}$, and $T = (y_{\Theta+2\pi} - y_{\Theta})/(x_{\Theta+2\pi} - x_{\Theta})$.

The three parameters W, T, and D define an enormous spectrum of possible shell forms, yet real shells are confined to a relatively small region of the parameter space (Figure 5.22). This concentration of observed forms can be understood to a large extent by considering some of the functional demands of bivalved and univalved organisms and their different modes of life.

In order for bivalved shells to articulate effectively, it is important to have a high expansion rate and low value of D (Figure 5.23). Deviations from this ideal, as in the upper part of Figure 5.23, would lead to extensive whorl overlap and therefore to interference between the two shells. The dashed lines in Figure 5.22 show the surface in the W–T–D space that separates shells with overlapping whorls from shells with open coiling. Bivalved shells, with nonoverlapping whorls, are confined to below this surface.

In fact, even having the appropriate values of W and D does not completely eliminate the problem of shell interference for bivalves. Figure 5.24a shows two shells with high W and low D superimposed. The umbonal regions of the two valves clearly interfere with each other in these model shells. There are at least three ways that bivalves can avoid shell interference. The first is to deviate from the ideal model by depositing extra shell material between the umbones, in effect to have a biological generating curve that is distinct from the geometric generating curve (Figures 5.24b and 5.24c). The second is to have valves that are distinctly unequal in size (Figure 5.24d). The third is to have equal valves with positive allometry of expansion rate, that is, a value of W that increases progressively with size (Figure 5.24e). The first and second strategies are widely exploited by both brachiopods and bivalve molluscs, while the third is most common in bivalve molluscs. The problem of valve interference is not always perfectly solved, however. A number of bivalve molluscs show beveled umbones caused by grinding together of the two valves.

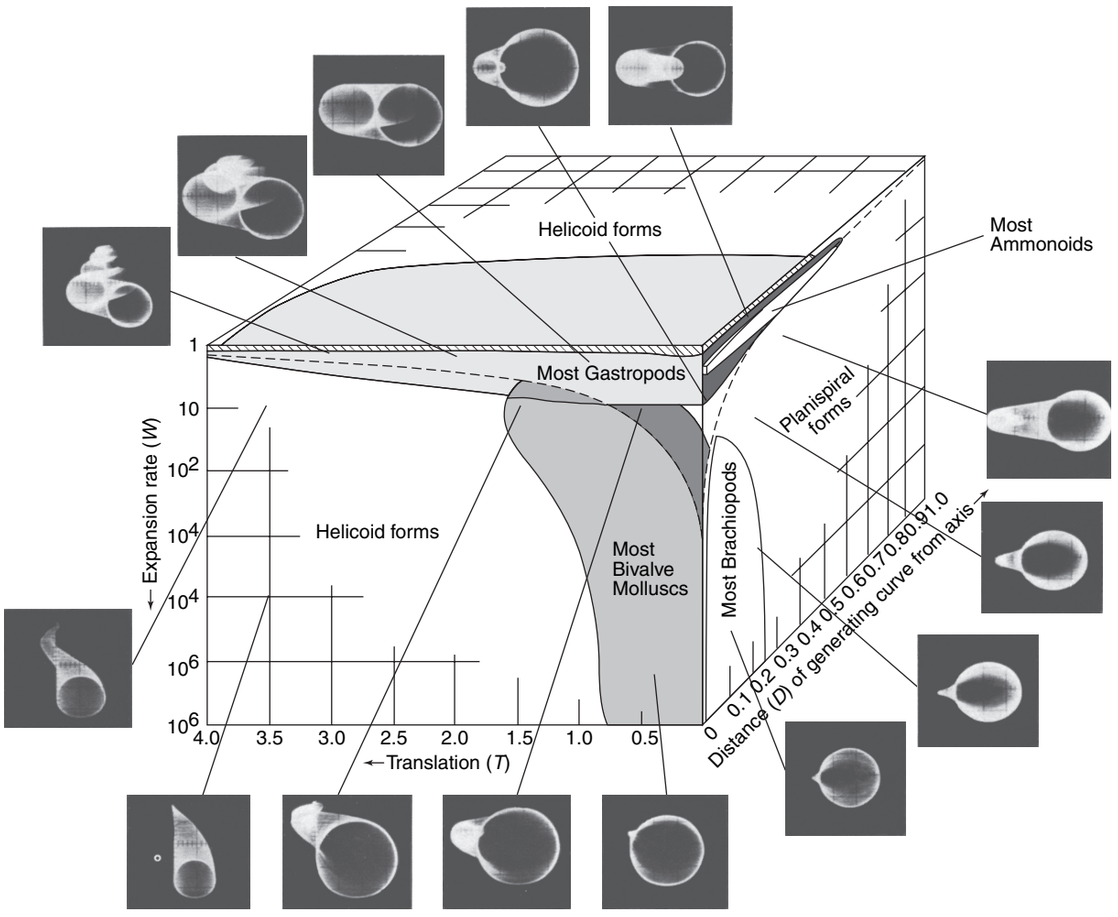

FIGURE 5.22 General distribution of observed forms within the theoretically possible coiling space. Representative computer-generated forms correspond to particular combinations of coiling parameters. Shaded areas show the combinations of coiling parameters typical of a few major taxonomic groups. Most of the theoretically possible space is not occupied by actual shells. The surface shown by the dashed lines separates shells with open coiling (below) from shells whose successive whorls overlap (above). *(From Raup, 1966)*

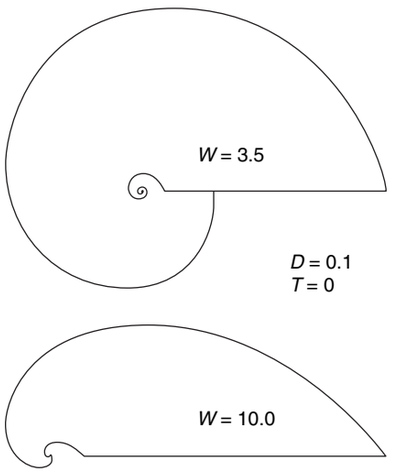

FIGURE 5.23 The effect of expansion rate on whorl overlap. A relatively low expansion rate yields whorl overlap, which is typical of univalves (top). A higher expansion rate produces no overlap, which is typical of each of the valves in a bivalve (bottom). *(From Raup, 1966)*

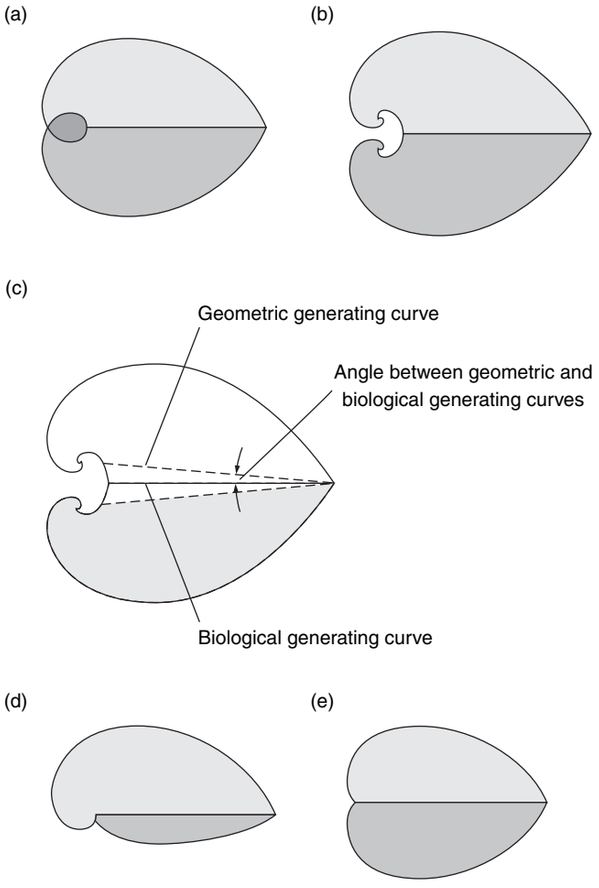

FIGURE 5.24 The problem of valve interference in bivalved shells. (a) The overlap in the umbonal region if both valves follow the ideal geometric model of coiling. (b) Interference is avoided by depositing additional shell material between the umbones. (c) Geometrically, this corresponds to having a biological generating curve, or actual growing shell margin, that is not the same as the geometric generating curve. The greater the angle between the biological and geometirc generating curves, the less the valves will interfere. Shell interference can also be avoided if the shells are highly unequal (d) or if whorl expansion rate increases during growth (e). *(a, b, d, e: From Ubukata, 2000; c: From Raup, 1966)*

The large apertures that characterize bivalved shells would be maladaptive for many univalves—such as snails—because this would make them highly susceptible to predation [SEE SECTION 9.4]. Univalves therefore tend to have relatively low values of W (Figure 5.22). In general, only univalves that gain protection by adhering completely to the substrate, such as abalones and limpets, can cope with a high expansion rate.

In addition, shells are stronger as successive whorls overlap more. Univalves tend to sit above the dashed surface of Figure 5.22. This means, as we saw in the discussion of bivalves, that their whorls overlap.

The projection of this surface onto the W–D plane, where $T = 0$, is a curve with the equation $W = 1/D$. Figure 5.25a depicts this curve along with a series of computer-generated shells that show closed coiling above the curve and open coiling below. For comparison, a sample of some 400 cephalopod genera is portrayed in Figure 5.25b. Estimates of W and D were obtained by measuring drawings and photographs of shells (see Box 5.2). The contour lines depict the density of occupation of the W–D space, with the concentration of points increasing toward the inner contour. These contours are thus two-dimensional analogs of frequency curves (see Box 3.1).

Almost all the observed shells fall in the region of closed coiling. However, even the species that fall on the other side of the curve in reality have closed coiling, as determined by inspection of the actual shells. As with any deviation between model and data, there are two possible reasons for the discrepancy. Either there is a problem with the data—namely, measurement error—or there is a problem with the model—for example, failure to take into consideration ontogenetic change in coiling parameters. In this case, it is likely that both factors play a role.

In summary, the coiling model can simulate the principal features of a wide range of shells with just three simple geometric parameters. Certain aspects of the nonrandom occupation of the parameter space can be understood in part by considering different ways of life and functional needs of organisms with coiled shells.

Trade-Offs and Limits to Optimality

A Model of Branching and Spiral Growth in Bryozoans Another large class of biological structures can be represented as a growing system of branches. These include circulatory systems, bacterial filaments, trees, antlers, crinoid arms, and the skeletons of some colonial invertebrates.

Suspension-feeding bryozoans have repeatedly evolved a form that combines helical growth along a main colony axis with the proliferation of lateral, branched extensions that contain feeding zooids (Figure 5.26). Such colonies can be modeled with a few simple

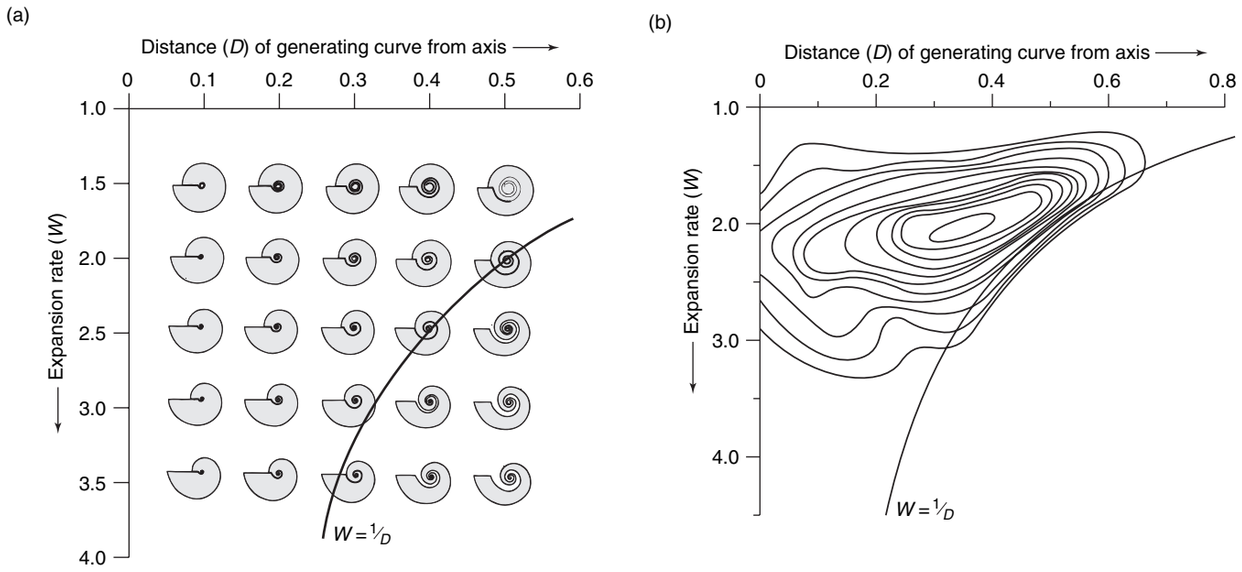

FIGURE 5.25 Hypothetical planispiral shells and measured ammonoids in *W–D* coiling space. (a) Hypothetical shells. $T = 0$ for shells that coil in a plane. (b) Measured shells. The contour lines show density of occupation of coiling space of a sample of about 400 ammonoid genera. The curve $W = 1/D$ separates openly coiled forms (below) from those with whorl overlap (above). *(From Raup, 1967)*

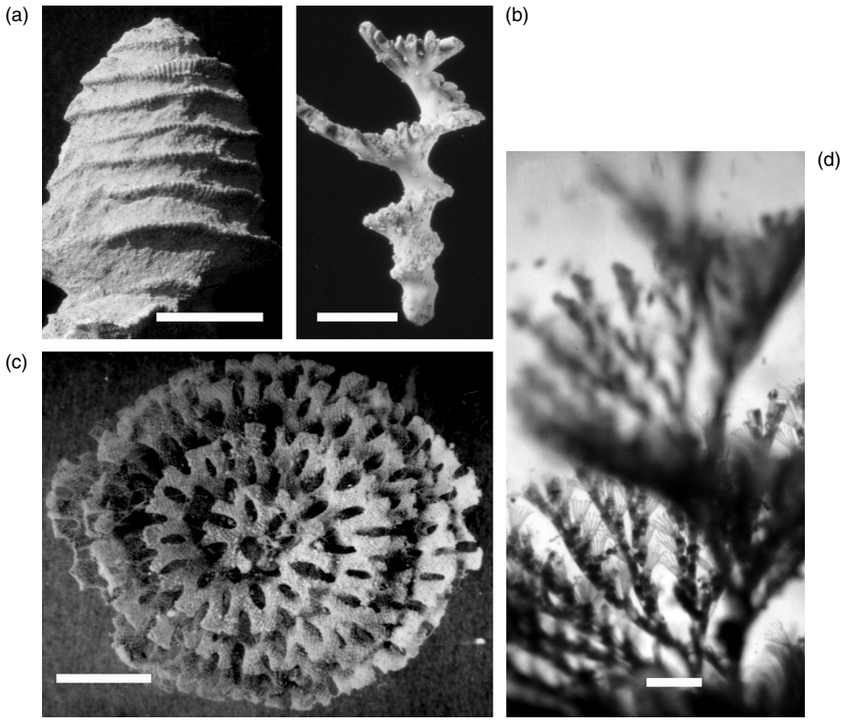

FIGURE 5.26 Examples of helically coiled, branching bryozoans. (a) *Archimedes* from the Carboniferous. (b) *Crisidmonea* from the Eocene. (c) *Retiflustra* from the present day. (d) *Bugula* from the present day. Scale bars are 10 mm in parts (a) through (c) and 1 mm in part (d). Part (c) is an axial view (see Figure 5.27a). Other views are lateral (see Figure 5.27b). *(From McGhee & McKinney, 2003)*

parameters (Figure 5.27): the radial distance between the coiling axis and the inner colony margin (*RAD*); the angular separation between innermost branches (*ANG*); the minimum distance between lateral branches (*XMIN*); the difference in elevation between lateral branches separated by 2π radians of revolution (*ELEV*); and the angle between a lateral branch and the coiling axis (*BWANG*). A wide spectrum of theoretically possible colony forms can be generated just by varying these last two parameters (Figure 5.28).

The mathematical model of colony form can be used to calculate the surface area of lateral branch systems corresponding to each combination of parameters. Contours in Figure 5.28 show values of surface area, increasing toward the lower left. The highest surface areas correspond to low values of both *ELEV* and *BWANG*. Because higher surface area of branches that possess feeding zooids would seem to allow greater food uptake, one

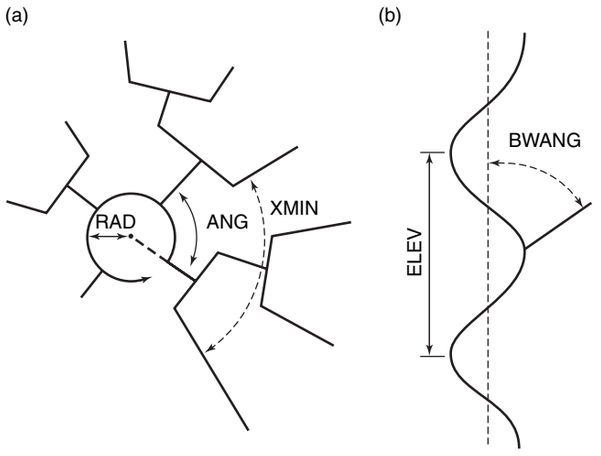

FIGURE 5.27 Geometric model of helical, branched bryozoans, showing five growth parameters. (a) View down the coiling axis. (b) Lateral view. *(From McGhee & McKinney, 2000)*

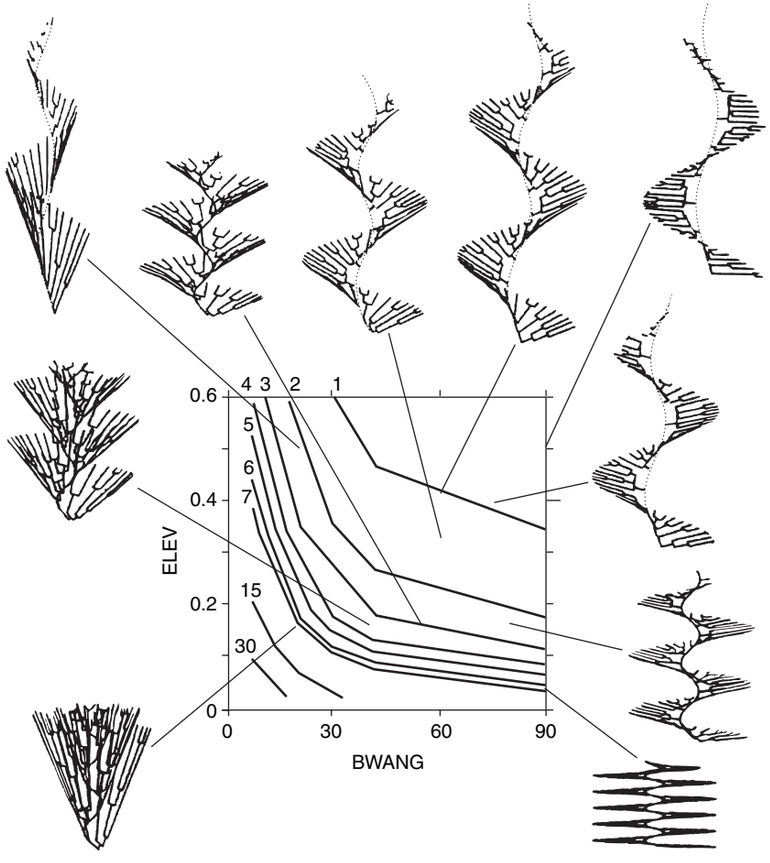

FIGURE 5.28 Effect of varying two of the parameters of the bryozoan model. Computer-generated forms correspond to particular parameter combinations. The lines inside the plot show contours of branch surface area, indicated by the numbers and increasing toward the lower left. *(From McGhee & McKinney, 2000)*

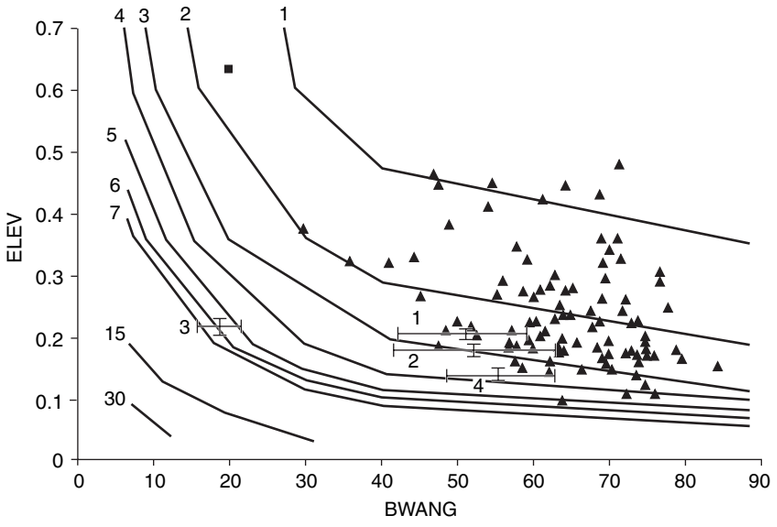

FIGURE 5.29 Distribution of observed forms in bryozoan model space. The axes and contour lines are as in Figure 5.28. The square shows a single specimen of the Devonian genus *Helicopora*. The triangles show multiple specimens of *Archimedes*. The numbered points with error bars show the mean and its standard error for three species of *Bugula* (1–3) and *Crisidmonea* (4). *(From McGhee & McKinney, 2000)*

might predict a concentration of bryozoan species in the lower left of this diagram. In fact, when real colonies are measured, they are found to be concentrated well away from this region (Figure 5.29).

The reason for the observed distribution of species can be understood by identifying an important trade-off. Based on observation of living helical bryozoans, it is known that water currents move through the colony from top to bottom, aided by the beating of cilia on bryozoan lophophores (feeding tentacles). As the water moves through the branches, it inevitably encounters resistance and slows down. Eventually it ceases to flow, producing a zone of stagnant water from which food cannot be extracted (Figure 5.30). Colonies with very low values of *ELEV* and *BWANG* would have deeply nested branches (Figure 5.28) and a correspondingly large stagnant zone. Thus, maximizing surface area makes feeding less efficient by increasing the size of the stagnant zone. The common colony forms represent a compromise that balances the need for feeding area with the need for fluid flow between the branches.

In the preceding example, the trade-off results, in essence, from a single functional demand—feeding—which is frustrated because the form that is optimal in terms of surface area is suboptimal in terms of fluid flow. We can gain further insight into the consequences of trade-offs by considering multiple functional demands that must be satisfied simultaneously (see Box 5.3). As the example of Box 5.3 shows, trade-offs between

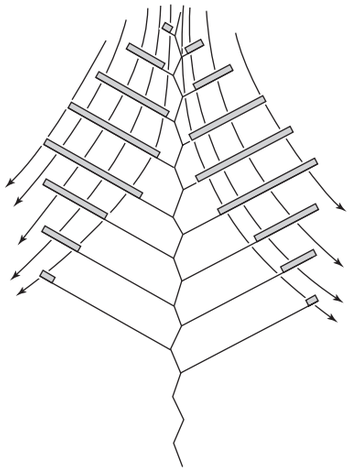

FIGURE 5.30 Schematic diagram showing feeding in the living bryozoan *Bugula*. The central line is the colony axis, and the radiating, thin lines show the branches. The thicker bars show the location of feeding zooids. The arrows indicate water flow; the area to the interior of these is a zone of relatively stagnant water. *(From McGhee & McKinney, 2000)*

Box 5.3

TRADE-OFFS AS A SOURCE OF MULTIPLE ADAPTIVE MODES

Figure 5.31 depicts a simple model of branching growth in land plants. There are three parameters: P, the probability of branching per unit branch length; ϕ, the angle between the two branches that diverge from a bifurcation; and γ, the angle of rotation between a new pair of branches and the branch from which it arises. Higher values of P yield more bifurcations and thus lead to more densely branched model plants. Higher values of ϕ give a wider divergence between branches. And higher values of γ produce new branches that are rotated more relative to their parent branch. The special case where $\gamma = 0$ would result in a plant restricted to a vertical plane.

There is thus a three-dimensional parameter space for branched plants in which the parameters have a definite theoretical range of values: P from 0 to 1; and ϕ and γ from 0° to 360°. Each point in this space specifies a different possible form. A very large but finite sample of the full spectrum of forms can be generated by varying each of the three parameters, in fine increments, over its entire range.

For certain functional demands, the performance of a theoretical form can be quantified. Therefore, all of the forms can be compared and the optimal ones can be identified. In this context, an optimum is a form that is functionally superior to all its neighbors in the parameter space. There can be multiple optima, and not all optima need to be equal in their functional performance. We confine this discussion to the biology that is relevant to the earliest vascular plants.

Consider first the single functional demand of reproduction. A spore can fall or be blown farther from the plant if it begins its descent from a greater height. Therefore, dispersal of spores will be maximized if plant height is maximized. At the same time, spores are produced at branch tips, so having more branches is advantageous in producing more spores. These two factors together lead to a single optimal phenotype, one that is very tall and has dense branching concentrated near the top (Figure 5.32a).

A second important function is the interception of light for photosynthesis. If performance is assessed with respect to this function alone, then there are three optima which differ in their details but share the property of numerous, broad, horizontal branches that enhance light capture (Figure 5.32b).

Finally, consider the function of mechanical stability. This correlates largely with the ability to resist bending. Resistance is highest when the plant is vertical, in other words, when ϕ is near zero (Figure

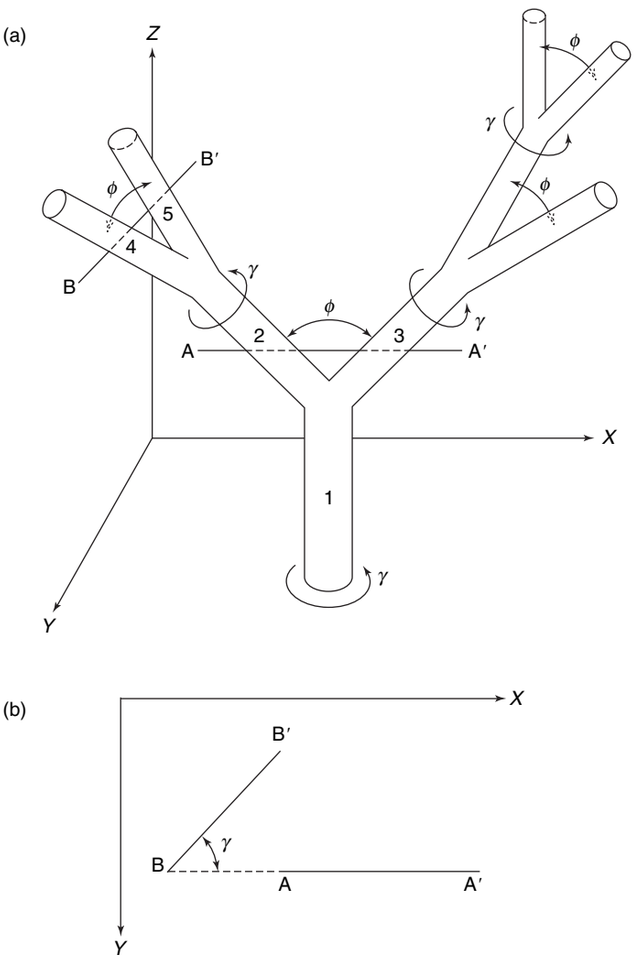

FIGURE 5.31 Geometric model of branching growth in plants. P is the probability of branching per unit branch length; ϕ is the angle between branches that arise from the same bifurcation; γ is the angle of rotation between the older and younger branches. (a) Branching in three dimensions. (b) The parameter γ. Line A–A′, between branches 2 and 3, and line B–B′, between branches 4 and 5, are projected into the x–y plane; γ is the angle between these projected lines. *(From Niklas & Kerchner, 1984)*

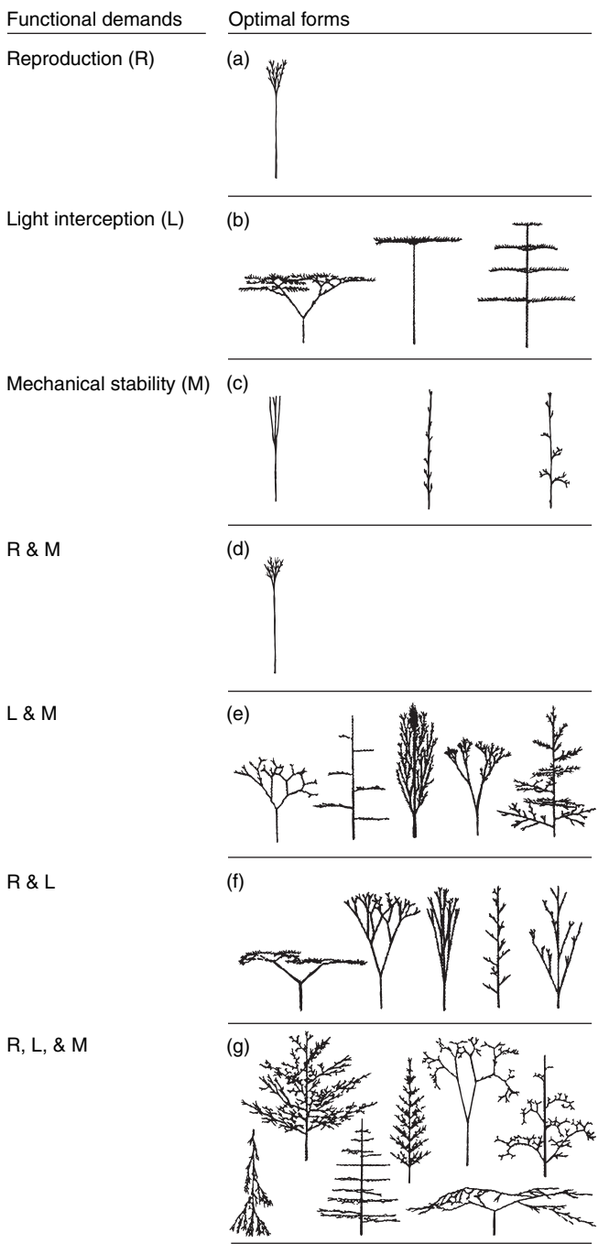

FIGURE 5.32 Optimal forms of model plants that satisfy different functional demands and combinations of demands. Because there are different ways to reach a compromise between conflicting demands, there are more distinct optima when more demands must be simultaneously satisfied. *(From Niklas, 1994)*

5.31). If stability alone needs to be maximized, then there are three distinct optimal forms (Figure 5.32c).

Of course, it is unrealistic to suppose that a plant has only a single function, so let us see what happens when there are multiple functional demands. Figure 5.32d depicts the single optimum that results when both reproduction and mechanical stability must be satisfied. In this case, there is not a serious trade-off because both functions are served by a tall, vertical structure. The single optimum that satisfies both functions is essentially the same as the one that satisfies reproduction only (Figure 5.32a).

Other combinations of functions are not so compatibile, however. Light interception, which favors horizontal branches, conflicts with mechanical stability, which favors vertical branches. Thus, the combination of functional demands forces compromises, leading to the several optimal forms of Figure 5.32e. Light interception and reproduction conflict for similar reasons, with results evident in Figure 5.32f.

One obvious result of conflicting demands is that there are more distinct optima than when there is a single function or two compatible functions. When conflicts are inevitable, there are many different ways to compromise. This is seen even more strikingly when all three functional demands are combined (Figure 5.32g). The increase in the number of distinct optima results from the different ways of balancing functions against one another. The fact that many of the plant forms of Figure 5.32 appear biologically realistic suggests that such trade-offs may indeed have been important in plant evolution and that the three functions explored here are among the most important for real plants.

incompatible functions are limitations in the sense that they prevent all aspects of performance from being maximized simultaneously. But they are also likely to contribute to the diversity of form, as evolution produces a variety of compromise solutions.

Phenotypic Change and Underlying Genetic Factors

An Alternative Model of Shell Coiling To the extent that models of form approximate growth processes, it may be possible to compare the size of a genetic change and the size of the corresponding phenotypic change. Differences in adult form that seem to the eye to be large may prove in some cases to involve a genetic or developmental change that is relatively small, and vice versa. A slight modification of the coiling model has been used to illustrate this principle.

In this variant of the shell coiling model, the growing margin is characterized by a field of vectors around the aperture (Figure 5.33). The orientation and length of the vectors show direction and rate of growth at each point. The vectors define the "aperture map" in which the shape of the resulting shell is encoded. A few aperture maps and their corresponding shells are shown in Figure 5.34. The shell in Figure 5.34a is a helical spiral typical of many snails; Figure 5.34c is a coiled, limpet-like shell, similar to the living *Crepidula*; and Figure 5.34b is intermediate between shells (a) and (c). An interesting feature of shells (a) through (c) is that they all have aperture maps with the same *relative* vector lengths; they differ only in absolute vector lengths.

Figure 5.34c differs from the shell of true limpets—for example, of the genus *Patella*—which resemble Figure 5.34d. The patelliform shell is practically a straight cone with no coiling. Its aperture map is very different from that of the coiled, limpet-like form.

Thus, there are at least two ways for a limpet form to grow, and therefore at least two ways to derive a limpet from a coiled ancestor such as the shell in Figure 5.34a. An evolutionary change that reduced all growth vectors by the same proportion could produce the transition from shell (a) to the limpet-like shell (c), because the aperture maps differ only in scale. By contrast, the transition to a conical limpet (d), with its unusual aperture map, would require an evolutionary change that affected different growth vectors disproportionately.

It is commonly thought that evolutionary transitions involving uniform change across many features of growth are more likely to occur than those in which different aspects of growth change by different amounts. If this is true, then the transition to the limpet-like form (Figure 5.34c) represents a smaller genetic change than the transition to the conical limpet (Figure 5.34d). This leads to a testable (but not yet fully tested) prediction: The evolution of coiled, limpet-like forms should have occurred more frequently in the history of gastropods than did the evolution of the conical limpet form. In this context, it is interesting to note that there are more species with the conical limpet form than with the coiled limpet-like form. This does not tell us, however, which form arose independently a greater number of times.

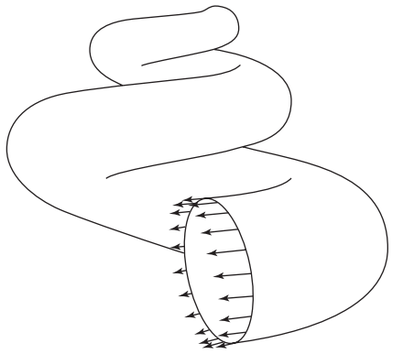

FIGURE 5.33 Alternative geometric model of shell growth. Each point on the margin has a rate and direction of growth, indicated by the length and orientation of the vectors (compare with Figure 5.19). *(From Rice, 1998)*

5.4 CONCLUDING REMARKS

Despite the successes of theoretical morphology, the range of taxonomic groups to which formal models have been applied is still relatively small. There is an obvious need for new ways to look at particular groups of organisms. A more important and far more elusive goal is to generate the theoretically possible spectrum of form of even more inclusive groups such as the animal and plant kingdoms. The model of plant growth considered in Box 5.3 is certainly an important step in this direction.

The questions and approaches discussed in this chapter apply as much to biology as to paleontology, and indeed functional morphology is a vibrant area of biological research. At the same time, the subject of theoretical morphology has received more attention from

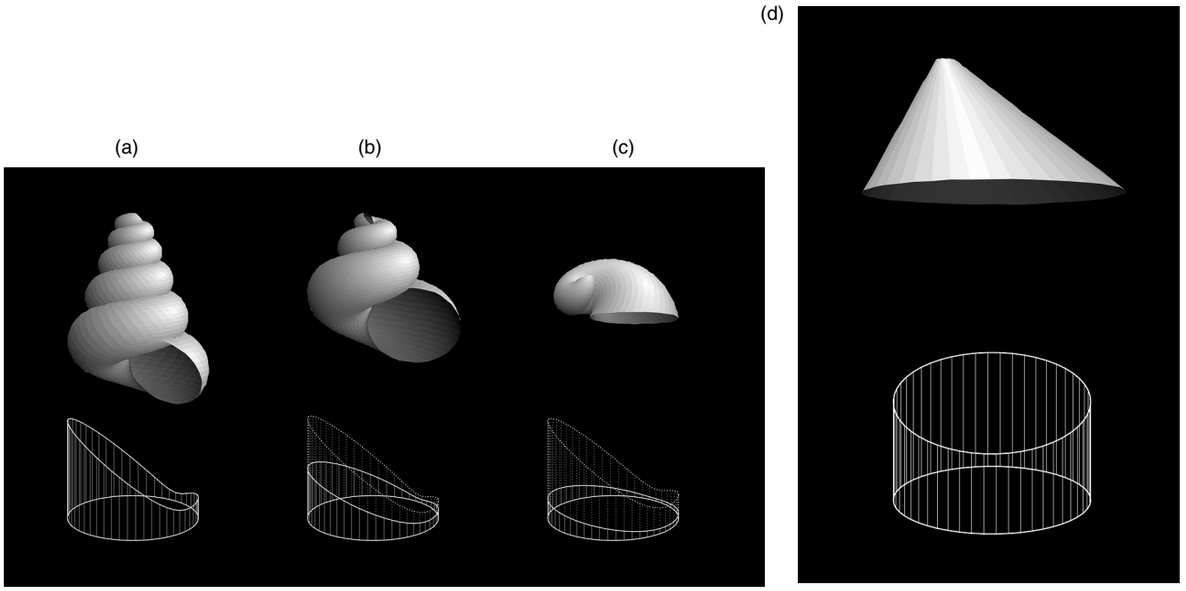

FIGURE 5.34 Comparison between three coiled shells and a conical limpet. (a) A high-spired, helically coiled form. (b) A form intermediate between parts (a) and (c). (c) A coiled limpet. (d) A conical limpet. The aperture maps below each computer-generated shell correspond to vector fields like the one in Figure 5.33; the length of each line segment is proportional to the rate of growth at a point on the margin. The dotted lines of maps (b) and (c) show the aperture maps of shells (b) and (c) magnified to a larger size. These magnified maps exactly match map (a). Therefore, it would be possible to derive (b) or (c) from (a) by a uniform scaling-down of the growth rates. The map of (d) is completely different from that of (a). Therefore, more substantial changes in the relative magnitudes of growth vectors would be required to derive (d) from (a). *(From Rice, 1998)*

paleontologists. There seem to be at least two reasons for this curious situation. First, paleontologists study fossil as well as living organisms, and therefore they must comprehend a broader diversity of form. Second, some of the first people to model morphology with the newly available computers in the late 1950s and early 1960s happened to be paleontologists, and their early work influenced later generations.

In this chapter, we have focused on adaptation in understanding individual forms. But this is only one of the three major determinants of form depicted in Figure 5.1. In fact, the relative importance of these three factors—that is, how much of the variance in form in the organic world can be attributed to each—is unknown. In a broader sense, our discussion of the overall distribution of form was also dominated by functional considerations. In Chapter 7, we consider rates of speciation and extinction as factors leading to the accumulation of species with particular morphologic features. These factors need not reflect adaptation.

SUPPLEMENTARY READING

Fisher, D. C. (1985) Evolutionary morphology: Beyond the analogous, the anecdotal, and the ad hoc. *Paleobiology* **11:**120–138. [Discussion of the principles underlying evolutionary morphology.]

McGhee, G. R. (1999) *Theoretical Morphology: The Concept and Its Applications*. New York, Columbia University Press, 316 pp. [Principles of theoretical morphology, with emphasis on paleontological examples.]

Plotnick, R. E., and Baumiller, T. K. (2000) Invention by evolution: Functional analysis in paleobiology. *Paleobiology* **26** (Suppl. to No. 4):305–323. [An overview of functional morphology in paleontology.]

Prusinkiewicz, P., and Lindenmayer, A. (1990) *The Algorithmic Beauty of Plants*. Berlin, Springer, 228 pp. [One of a series of volumes exploring theoretical morphology through systems that generate form by replicating basic elements according to simple rules.]

Radinsky, L. (1987) *The Evolution of Vertebrate Design*. Chicago, University of Chicago Press, 188 pp. [Mechanistic description of vertebrate function.]

Rudwick, M. J. S. (1964) The inference of function from structure in fossils. *British Journal for the Philosophy of Science* **15:**27–40. [Landmark paper on the application of engineering principles to functional morphology in paleontology.]

Savazzi, E. (ed.) (1999) *Functional Morphology of the Invertebrate Skeleton*. Chichester, U.K., Wiley, 706 pp. [Case studies of functional morphology in living and fossil invertebrates.]

Thompson, D'A. W. (1942) *On Growth and Form*. Cambridge, U.K., Cambridge University Press, 1116 pp. [Includes consideration of structural factors that contribute to biologic form.]

Thompson, J. J. (ed.) (1995) *Functional Morphology in Vertebrate Paleontology*. Cambridge, U.K., Cambridge University Press, 293 pp. [Case studies of functional morphology in fossil vertebrates.]

Vogel, S. (1981) *Life in Moving Fluids*. Princeton, N.J., Princeton University Press, 352 pp. [Principles of fluid dynamics applied to fluid flow within organisms and to the function of organisms in water and air.]

Wainwright, S. A., Biggs, W. D., Currey, J. D., and Gosline, J. M. (1976) *Mechanical Design in Organisms*. Princeton, N.J., Princeton University Press, 423 pp. [Engineering principles applied to organisms, with particular emphasis on structural properties of biological materials.]